**Earth System
Dynamics
Discussions**

A synthesis of climate-based emission metrics with applications

B. Aamaas, G. P. Peters, and J. S. Fuglestvedt

Center for International Climate and Environmental Research – Oslo (CICERO),
PB 1129 Blindern, 0318 Oslo, Norway

Correspondence to: B. Aamaas (borgar.aamaas@cicero.uio.no)

Title Page

Abstract	Introduction
Conclusions	References
Tables	Figures

|◄ | ►|
◄ | ►
Back | Close

Full Screen / Esc

Printer-friendly Version

Interactive Discussion

Abstract

In the context of climate change, emissions of different species (e.g. carbon dioxide and methane) are not directly comparable since they have different radiative efficiencies and lifetimes. Since comparisons via detailed climate models are computationally expensive and complex, emission metrics were developed to allow a simple and straight forward comparison of the estimated climate impacts of the emissions of different species. Because emission metrics depend on a variety of choices, a variety of different metrics may be used and with different time-horizons. In this paper, we present analytical expressions and describe how to calculate common emission metrics for different species. We include the climate metrics radiative forcing, integrated radiative forcing, temperature change, and integrated temperature change in both absolute form and normalized to a reference gas. We consider pulse emissions, sustained emissions, and emission scenarios. The species are separated into three types: species with a simple exponential decay, CO_2 which has a complex decay over time, and ozone precursors (NO_x, CO, VOC). Related issues are also discussed, such as deriving Impulse Response Functions, simple modifications to metrics, and regional dependencies. We perform various applications to highlight key applications of simple emission metrics, which show that emissions of CO_2 are important regardless of what metric and time horizon is used, but that the importance of SLCFs varies greatly depending on the metric choices made.

1 Introduction

Multicomponent climate policies require a method to compare the climate impact of emissions of different species (Fuglestvedt et al., 2003). While it is most common to compare different long-lived greenhouse gases (LLGHGs), e.g., CO_2 and CH_4, it may also be useful to compare short lived climate forcers (SLCFs), e.g. black carbon (BC) and organic carbon (OC), and to compare LLGHG and SLCF, e.g., CO_2 and BC.

Different species have different radiative efficiencies and remain in the atmosphere over different time scales (Forster et al., 2007). Thus, a direct comparison of species by weight does not correlate with the climate impact.

It is common to compare emissions in terms of Radiative Forcing (RF), and most emission metrics use RF as a starting point. A limitation of using RF directly is that it does not capture the transient response in the atmospheric concentration when medium to long-lived gases are studied. The most common emission metric used today is the Global Warming Potential (GWP), which compares the integrated RF of a pulse emission of a given species relative to the integrated RF of a pulse emission of CO_2. Thus, the GWP captures some transient features of the RF of different species by integrating over time. The GWP was originally proposed as an "illustrative example" in the IPCC First Assessment Report (IPCC, 1990) and has since been critiqued from many angles (Fuglestvedt et al., 2003; Manne and Richels, 2001; Manning and Reisinger, 2011; Shine, 2009; Victor, 1990; Fuglestvedt et al., 2000; Smith and Wigley, 2000a, b), particularly related to its interpretation. In response to the critiques of the GWP, several alternatives have been proposed. The next most common metric in use today is the Global Temperature change Potential (GTP) (Shine et al., 2005, 2007). The GTP compares the temperature change at a point in time due to a pulse emission relative to the temperature change due to a pulse emission of CO_2. The GTP combines the temporal change in the RF of different species with the temporal behavior of the temperature response of the climate system, thus, going beyond a key limitation of the GWP. Various other emission metrics have been proposed (see Tanaka et al., 2010, for a review), but these are in less common usage.

All of the IPCC Assessment Reports have had a section on emission metrics (IPCC, 1990, 1995, 2001, 2007), and several other IPCC related reports have contributed additional background information (Isaksen et al., 1992; IPCC, 1994; Enting et al., 1994). In addition to updating the scientific progress on emission metrics, each new IPCC report generally updates radiative efficiencies and atmospheric lifetimes. However, it is, in general, not always transparent what assumptions and equations are used for

metric estimates. The motivation for this paper is to present the relevant background, key assumptions, and equations used to estimate emission metrics. While the metric equations are not new (Fuglestvedt et al., 2010; Peters et al., 2011a), here we combine them together in a consistent framework and provide ancillary information on their interpretation and application.

2   Metric overview and equations

Emission metrics can be used in several ways (Fuglestvedt et al., 2003; Tanaka et al., 2010), but the main ways are to (1) compare the climate impacts of the emissions of different species to gain greater scientific understanding (e.g. Collins et al., 2010; Shindell et al., 2009), (2) provide an "exchange rate" on how to weight the emissions of different species for mitigation policies, as in the Kyoto Protocol (Skodvin and Fuglestvedt, 1997), and (3) perform comparisons of different activities and technologies that emit species at different rates such as in Life Cycle Assessment (LCA) (Peters et al., 2011b; Pennington et al., 2004; Boucher and Reddy, 2008; Tanaka et al., 2012). Due to the variety of applications, there is no obvious need to have one single metric for all applications, and a range of different metrics may even be used in one application. Thus, it is worthwhile to start with a general formulation of an emission metric (Kandlikar, 1996; Forster et al., 2007)

$$AM_i = \int_0^{TH} [(I(\Delta C_{r+i}(t)) - I(\Delta C_r(t)))g(t)]dt \tag{1}$$

where $I(\Delta_i(t))$ is a function describing the "impact" of a change in climate (e.g., concentration, temperature, precipitation), ΔC, at time t, with a discount function, $g(t)$, and compared to a reference system, r, on which the perturbation occurs, i. The discount function can represent a fixed time-horizon using a step-function (such as in most integrated metrics like the GWP), instantaneous evaluation using a Dirac delta function

(such as in most end-point metrics like the GTP), or a more common exponential function as often used in economics. Fuglestvedt et al. (2003) estimated exponential discounting functions to replicate the use of step-function for a fixed time-horizon, but found that different species had different discount rates. A Dirac delta function for end-point metrics has the function of removing the integral and evaluating the integral at the time horizon. The time horizon, TH, can take any value between 0 and infinity.

For the different applications of emission metrics, either an absolute metric (AM) or normalized metric (M) is used. To compare two emission perturbations i and j, the climate impact can be compared as a function of time using AM_i and AM_j. A normalized metric

$$M_i(t) = \frac{AM_i(t)}{AM_j(t)} \tag{2}$$

is made relative to a reference gas (j), usually CO_2, and puts the emissions of two components into the same units, usually called "CO_2-equivalent emissions." The normalized metric value can be considered as a conversion factor from the unit of the emission (e.g., kg CH_4) to the "equivalent" emission of CO_2 that would ideally lead to the equivalent climate impact for the given TH and underlying assumptions; $E_j(CO_2$-eq) $= E_j \cdot M_j$. The choice of reference gas is difficult, and the long term behavior of CO_2 is one of the main reasons for needing a value-based TH in normalized emission metrics (IPCC, 1990; Lashof and Ahuja, 1990). Several studies have also used a time-varying TH, where the TH changes as it moves towards a target year (TE), TH = TE – t (Shine et al., 2007). The time-varying metric shows the characteristic features of many emission metrics from the economic literature (Manne and Richels, 2001; Johansson, 2012).

We develop the different emission metrics based around the use of Eq. (1). While seemingly abstract, the application of Eq. (1) can be applied by following some simple steps, and here we give an illustrative example of concentration and RF. An emission into the atmosphere leads to an increase in the atmospheric concentration of that component. The atmospheric concentration decays dependent on the efficiency that the

species is removed from the atmosphere, which is described by an impulse response function (IRF). Due to chemical reactions in the atmosphere, some emissions of one type of component can lead to an increase or decrease in the concentration of another type of component (e.g., ozone precursors). While the species is resident in the atmosphere, the increased atmospheric concentration of the species causes an additional RF, which for emission metrics is usually expressed in a linearized form using the radiative efficiency (RE). A RF can also be caused by indirect effects (e.g., aerosol effects on clouds). The response considered in the metrics is governed by the temporal evolution of the RF, which is dependent on the RE and removal rate from the atmosphere leading to $\Delta C(t)$. The response can be directly related to the RF, or additional models can be used to quantify the climate impact desired. All these terms are explained further below.

The equations presented here are an extension of work in the ATTICA project (Fuglestvedt et al., 2010), but with a more thorough description and derivation of the formulas and discussion of the assumptions. All the parameters used in the metrics are defined in Table 1. The notation is slightly different to Fuglestvedt et al. (2010); we have avoided a mixed use of subscripts and superscripts, we use τ as the species' lifetime instead of as α to avoid confusion with the parameter a in the Impulse Response Function (IRF). We develop the equations for emission pulses as this is most common for emission metrics, since these can be used as building blocks for other applications. However, we later discuss the equations and results for sustained emissions and emission scenarios.

2.1 Impulse Response Function (IRF)

Once pollutants are emitted into the atmosphere, the pollutants will initially increase the atmospheric concentration before gradually being removed from the atmosphere leading to a decrease in concentration. In simple representations, the removal from the atmosphere for a pulse emission can be represented by a single or a sum of exponentials. Exponentials are particularly useful as they can be easily used in convolutions to

represent the behavior of arbitrary emissions scenarios (Enting, 2007; Wigley, 1991), be converted into a set of differential equations for efficient solutions (Wigley, 1991), and in some cases the time scales in the IRF have physical interpretations (Li and Jarvis, 2009; Li et al., 2009). Most species can be represented by a single exponential (time-scale), though CO_2 is usually represented using multiple exponentials (time-scales) (Forster et al., 2007).

2.1.1 Multiple time-scales (CO_2)

For CO_2, the IRF is usually represented with multiple time scales (Archer et al., 2009), and it is assumed a fraction remains in the atmosphere indefinitely,

$$\text{IRF}_{CO_2}(t) = a_0 + \sum_{i=1}^{I} a_i \exp\left(-\frac{t}{\tau_i}\right) \tag{3}$$

where $\Sigma a_i = 1$. The decay of CO_2 does not reach zero at infinity with existing IRFs, as opposed to the other species. This is a result of the non-linear kinetics of the CO_2 perturbation, slow deep ocean circulation, and slow uptake of CO_2 in the land reservoir on geological timescales. The literature suggests that "about 50 % of an increase in atmospheric CO_2 will be removed within 30 yr, a further 30 % will be removed within a few centuries and the remaining 20 % may remain in the atmosphere for many thousands of years" (Archer et al., 2009; IPCC, 2007). As the climate changes, the IRF will also change, as land and ocean will take up less CO_2 in a warmer climate (Friedlingstein et al., 2006).

The IRF for CO_2 that is used in emission metrics is calculated based on the Bern carbon cycle model (Joos et al., 2001) with the IRF experimental setup described by Enting et al. (1994), also see Fig. 1 in Joos et al. (2012). In the specific case of the Fourth Assessment Report (IPCC, 2007), the IRF was estimated based on a two-step process, a control and perturbation run. First, for the control, the carbon cycle model is run with historical emissions until 2005, and from 2005 the emissions are calculated

to keep a constant CO_2 concentration. Second, in the perturbation run, the emissions from the control are used but a large pulse emission (40 GtC) is placed in 2010 and the model is allowed to run until near equilibrium. The IRF is based on the normalized version of the difference between the perturbation and control run, after which a sum of exponentials is fitted. The decay parameterization is not directly linked to any processes; however, the scales can be loosely interpreted as the uptake in land biosphere and the surface layer of the ocean for the short and medium time scales, the surface layer mixing with the deep ocean for the long time scales, and the slow geological processes representing the infinite time scale (Archer and Brovkin, 2008; Archer et al., 2009; Li et al., 2009).

Uncertainties in the carbon cycle and in the experimental set up, both have a large effect on the IRF (Wuebbles et al., 1995; Enting et al., 1994; Reisinger et al., 2010; IPCC, 1994; Archer et al., 2009; Eby et al., 2009). Different carbon cycle models lead to large differences in the air-borne fraction after 500 yr (up to 0.2) and also the decay parameters in the IRF (IPCC, 1994, Fig. 5.4; Enting et al., 1994, Fig. 9.1; Archer et al., 2009). Carbon cycle feedbacks can also lead to a large spread in the response of the carbon cycle (Friedlingstein et al., 2006) and consequently metric values (Gillett and Matthews, 2010). Reisinger et al. (2010) estimated the uncertainty associated with CO_2 to be about 25 % for AGWP-100 and about 35 % for AGTP-20.

The Bern Carbon Cycle model was used for the IRF in IPCC reports (see Enting et al., 1994, Sect. 9b), and the use of one model may give biased results compared to a model ensemble. Figure 1 shows the IRFs from the first four IPCC assessment reports. In SAR, TAR, and AR4, the Bern Carbon Cycle was used, though each time it was improved making it difficult to determine if variations are due to model differences or changes in the background concentration. Using an experimental set up with a constant or scenario background to calculate the IRF, can lead to a difference in the air-borne faction of 0.1–0.2 after 500 yr (IPCC, 1994, Fig. 5.5; Enting et al., 1994, Fig. 9.1 and 9.2). In addition, the IRF will change depending on time the pulse is released in the experimental set up (IPCC, 1994, Fig. 5.5). Different pulse sizes also lead to different

Title Page

Abstract | Introduction

Conclusions | References

Tables | Figures

◄◄ | ►►

◄ | ►

Back | Close

Full Screen / Esc

Printer-friendly Version

Interactive Discussion

IRFs (Archer et al., 2009). Thus, the background, and its evolution, is an important determinant in the calculation of the IRF. The experimental set up used in the IPCC reports is not meant to represent a realistic situation, but rather a simple and constant background on which to allow transparent comparisons (Enting et al., 1994; IPCC, 1994). A recent model intercomparison shows that the response of the Bern model is similar to the model mean (Joos et al., 2012), as was the case for an earlier version of the Bern model (Enting et al., 1994).

2.1.2 Single time-scales (everything other than CO_2)

Most other species are assumed to follow a simple exponential decay with one time-scale:

$$\text{IRF}_x(t) = \exp\left(-\frac{t}{\tau}\right) \tag{4}$$

Though, in practice, the decay may happen on different time scales for different processes, and, thus, the atmospheric adjustment time may differ from the residence time (Prather, 2007). These physical processes leads to what is usually called "indirect effects" (e.g. Forster et al., 2007). Since these indirect effects influence the lifetime and effects of species, we mention several examples here. For example, N_2O removal in the atmosphere is mainly due to photolysis and reaction with meta-stable $O(^1D)$, both in the stratosphere (Prather, 2007). Particles, such as black carbon, are removed by wet and dry deposition, hence the process can be strongly regionally dependent (Shindell and Faluvegi, 2009; Berntsen et al., 2006). CH_4 is removed from the atmosphere from three processes (Boucher et al., 2009): (1) around 88 % is removed by reacting with hydroxyl radicals in the troposphere, (2) 7 % is destructed in the stratosphere, and (3) 5 % is removed by bacteria in the soil. These three processes act on different time scales, but can be represented by one time scale by connecting a system of first order differential equations leading to the adjustment time

$$\frac{1}{\tau} = \frac{1}{\tau_1} + \frac{1}{\tau_2} + \frac{1}{\tau_3} \tag{5}$$

The common ozone precursors (NO_x, CO, VOC) used in emission metrics are based on more detailed calculations and this is discussed in more detail below. Uncertainties in the lifetimes are due to uncertainties in the emission estimates and atmospheric chemistry (Prather et al., 2012).

2.1.3 Temperature

For emission metrics that link from RF to temperature, an IRF is needed for the temperature response to an instantaneous unit pulse of RF, IRF_T. A simple exponential parameterization is usually used,

$$IRF_T(H) = \sum_{j=1}^{J} \frac{c_j}{d_j} \exp\left(-\frac{H}{d_j}\right) \tag{6}$$

where the c add to give the climate sensitivity and d are the corresponding time scales. IRF_T can be mapped to a simple box-diffusion energy balance model, which aids in its interpretation (Peters et al., 2011a; Li and Jarvis, 2009). The exponential term with the shortest time scale maps to the mixed atmosphere-ocean later, the next largest time scale maps to the next deepest ocean layer and so on. The climate sensitivity can be determined by estimating the equilibrium response to a step (sustained) RF,

$$\lambda = \int_0^\infty IRF_T(t)\,dt = \sum_{j=1}^{J} c_j \tag{7}$$

The parameters for IRF_T are usually calculated as a response in the global temperature to a pulse of RF, or experiments that allow a pulse to be estimated such as the

C3MIP and C5MIP 1 % increasing CO_2 emission scenarios (Olivié et al., 2012). Most temperature based emission metrics use an IRF based on the Hadley model (Boucher and Reddy, 2008) response to a 1 % yearly increase in CO_2 emissions until 70 yr after which the concentration is held constant until 1000 yr. The parameters are derived from a curve fit to the results.

Recently, Olivié et al. (2012), estimated IRF_T for a range of models from the CMIP3 collection, Fig. 2, which indicates the model spread and dependence on experimental set up. It is clear that using a single exponential term does not give a realistic response compared to using 2 or 3 exponential terms to the RF, a similar conclusion was found by Li and Jarvis (2009). For the CMIP3 experiments, with relatively short integrations of 100–300 yr, two exponential terms are sufficient (Olivié et al., 2012), but for longer simulations three terms may be more representative (Li and Jarvis, 2009). The differences between the Hadley model and the CMIP3 ensemble, Fig. 2, represents both model variations and different integration lengths, with the Hadley model integrated to 1000 yr.

The short integrations in CMIP3 make it difficult to estimate the longer time constant, and, hence, the climate sensitivity derived from the IRFs differs from the climate sensitivity of the climate model (Olivié et al., 2012). This raises the question of how reliable the IRFs are, and whether they should be modified to match the correct climate sensitivity of each model. As argued elsewhere (Olivié et al., 2012), the IRF is the best fit to a curve and the solution space is flat leading to a large spread in (equally) good estimates if the IRF. Consequently, not too much should be interpreted from the parameters of the IRF.

There are relatively few IRF_T currently available for different models (with recent exceptions, Olivié et al., 2012). It is possible, however, to modify IRF_T of one model to match some aspects of another model, for example, the climate sensitivity. If the time constants of the IRF_T are assumed to be fixed, then the climate sensitivity can be scaled to match another model using a uniform scaling (e.g., $IRF_{T,\text{new}} = \lambda_{\text{new}} \times IRF_T / \sum c$, see Eq. 6). However, in reality, a different climate model is likely to

have different time scales (Olivié et al., 2012). That is, the IRF parameters are not independent (Li and Jarvis, 2009; Peters et al., 2011a; Berntsen and Fuglestvedt, 2008) and, hence, modifying the components of the climate sensitivity also modifies the time scales. Figure 3 shows the result of a simply scaling of the Hadley IRF to have a climate sensitivity of 0.8, a process which simply shifts the IRF vertically. If a two-layer box-diffusion model (Peters et al., 2011a) is based on the parameters of the Hadley model (specific heat capacities and vertical diffusivity), but the climate sensitivity of 0.8, then the IRF is different (Fig. 3) and the time scales change from 8.4 yr to 7.0 yr and 409.5 yr to 369.0 yr. This process assumes the specific heat capacities and vertical diffusivity are the same for the given λ, which is unlikely to be true. Thus, a better approach is to estimate an IRF for the specific climate model (Olivié et al., 2012).

2.2 Radiative efficiencies

Once a species is in the atmosphere and contributes to an increase in the atmospheric concentration of that component, it causes a radiative imbalance of energy into the earth system. The RF is usually calculated by complex radiative transfer models (Forster et al., 2007), but for emission metrics simplifications are usually made based on the current state of the atmosphere. The RF is defined as the change in net irradiance at the tropopause after allowing for stratospheric temperatures to readjust to radiative equilibrium, while surface and tropospheric temperatures and state are held fixed at the unperturbed values (IPCC, 2001; Hansen et al., 2005). The RE is a linearization of the non-linear RF and is defined as the RF due to a unit increase in the concentration of a trace gas (IPCC, 1990). In this section, we discuss different ways to calculate the RE and demonstrate the differences with examples for CO_2.

In many papers, the RE is shown in $W\,m^{-2}\,ppb^{-1}$, while for calculations it is necessary to use $W\,m^{-2}\,kg^{-1}$. The conversion factor from ppb to kg is

$$C_X\,(\text{kg}) = \left(\frac{M_A}{M_X}\right) \times \left(\frac{10^9}{T_M}\right) \times C_X(\text{ppb}) \tag{8}$$

where M_A is the mean molecular weight of air ($28.96\,\text{kg}\,\text{kmol}^{-1}$), M_X molecular weight of molecule X, and T_M total mass of the atmosphere ($5.15 \times 10^{18}\,\text{kg}$) (Shine et al., 2005).

2.2.1 Carbon Dioxide (CO_2)

The RF for CO_2 can be approximated using the expression based on radiative transfer models (Myhre et al., 1998),

$$\text{RF} = \alpha \ln \left(\frac{C_0 + \Delta C}{C_0} \right) \tag{9}$$

where C_0 is the unperturbed atmospheric concentration of CO_2, ΔC is a perturbation over C_0, and $\alpha = 5.35$ is a constant. Forster et al. (2007) assessed this equation to be accurate within 10 %. Since emission metrics are often based on a constant background concentration, the RE is often taken as constant, for example, based on C_0 in 2005 for IPCC AR4 (Forster et al., 2007). For scenarios, the RE will change as a function of time, though the changes are partially offset by changes in the IRF as a function of time (Caldeira and Kasting, 1993; Reisinger et al., 2011). The RE can be evaluated as an average or marginal estimate (e.g., Huijbregts et al., 2011).

Average: IPCC (2007) estimates the RE of CO_2 "for a small perturbation" of CO_2 from the current unperturbed concentration, C_0 (Forster et al., 2007)

$$A_{CO_2,\text{average}} = \alpha \ln \left(\frac{C_0 + \Delta C}{C_0} \right) / \Delta C \tag{10}$$

where the small perturbation, ΔC, is taken as 1 ppm (Forster et al., 2007), though it is not clear why 1 ppm is chosen. WMO (1999) used for IPCC TAR states ΔC "is magnitude of the CO_2 pulse in ppmv".

Marginal: The RE can also be calculated by taking the derivative of RF_{CO_2} to consider the marginal change (Caldeira and Kasting, 1993; Lelieveld and Crutzen, 1992)

$$A_{CO_2, \text{ marginal}} = \left. \frac{d(RF)}{d(\Delta C)} \right|_{\Delta C=0} = \frac{\alpha}{c_0} \qquad (11)$$

This is equivalent to taking $\Delta C \rightarrow 0$ in the average approach.

Earlier IPCC assessment reports do not state the method of estimating the RE, and it is not clear what the difference between different estimates may be. A schematic comparison of the two methods is shown in Fig. 4, while the numerical differences are presented in Table 2. Taking an average with a Δc step of *1 ppm* (similar to the pulse size of 10 GtC used for the SAR and TAR IRFs, Enting et al., 1994), the difference with the marginal estimate is negligible (about 0.1 %). The difference increases almost linearly with increasing step size (Table 2). The difference per ppm also decreases, as the background concentration c_0 increases. These differences are much smaller than, for example, the uncertainties in the RF of LLGHGs, which is estimated to be 10 % (Forster et al., 2007). While the differences may be small, it would nevertheless be useful to have a more explicit and less ambiguous definition of radiative efficiency.

An additional issue is whether it is desirable, for impact assessment, to rebase the RE to the most recent atmospheric concentration (e.g., Huijbregts et al., 2011). As c_0 increases, the RE decreases and, hence, CO_2 becomes relatively less important. For impact assessment, it is unclear whether it is intended, or desirable, for the RE to decrease by constantly changing c_0. One could argue, for example, to have c_0 taken as the preindustrial concentration and use a marginal value (e.g., Huijbregts et al., 2011). In the case of CO_2, the RE in 2005 is 40 % lower than pre-industrial times and may be 50–100 % lower in 2100 depending on the future scenario (Fig. 5). For consistency with the RE, the IRF could also be based on preindustrial conditions. This would avoid the problem of IRF, RE, and, hence, emission metrics changing as a function of time (Wuebbles et al., 1995; Caldeira and Kasting, 1993; Reisinger et al., 2011; Enting et al., 1994).

2.2.2 Methane (CH_4), Nitrous Oxide (N_2O), and other LLGHGs

The RF estimates of CH_4 and N_2O are based on radiative transfer models (IPCC, 2001; Myhre et al., 1998),

$$RF_{CH_4} = \alpha_{CH_4} \left(\sqrt{M} - \sqrt{M_0} \right) - \left[f(M, N_0) - f(M_0, N_0) \right] \tag{12}$$

and N_2O is calculated by

$$RF_{N_2O} = \alpha_{N_2O} \left(\sqrt{N} - \sqrt{N_0} \right) - \left[f(M_0, N) - f(M_0, N) \right] \tag{13}$$

where $\alpha_{CH_4} = 0.036$ and $\alpha_{N_2O} = 0.12$, M is the CH_4 concentration in ppb and N is the N_2O concentration in ppb, and the subscript 0 denotes the unperturbed concentration. The function f is

$$f(M, N) = 0.47 \ln \left[1 + 2.01 \times 10^{-5} (MN)^{0.75} + 5.31 \times 10^{-15} M (MN)^{1.52} \right] \tag{14}$$

Further, the specific forcing of CH_4 is increased by a factor 1.4, due to effects on tropospheric ozone and stratospheric water vapor (IPCC, 2001; Forster et al., 2007).

The RE is based on these equations, however, as for CO_2, there is ambiguity in how to estimates the RE; marginal or average. As for CO_2, it is also straightforward to estimate the radiative efficiency of CH_4 and N_2O using the derivative of the above expressions.

The RE for other LLGHGs with low atmospheric concentrations, such as hydrochlorofluorocarbons and hydrofluorocarbons, are calculated from the linear increase in RF based on the measured infrared absorption spectra of those species (Pinnock et al., 1995; Hodnebrog et al., 2012).

2.2.3 Short-Lived Climate Forcers (SLCFs)

The RE for short-lived components is based on chemical transport models and RF calculations (Fuglestvedt et al., 2010). The common approach to calculate the RE is to

run a model perturbation which reduces the emissions by a fraction of one species at a time and then calculates the difference in radiative balance between this perturbed case and the reference simulation (Fuglestvedt et al., 2008; Forster et al., 2007). The RE is, then, calculated as the ratio between the calculated RF and change in burden. For some SLCFs, there are some non-standard issues in calculating the RE and the main ones are now explored.

Estimating A_x for SLCF with adjustment times significantly less than one year

When the lifetime of the SLCF is significantly less than one year (e.g., a week or less), then some papers calculate the RF at $t = 1$, RF_{SS}, based on steady state emissions of the SLCF (Fuglestvedt et al., 2008). The main reason for using this method is that it provides an annual averaged value. RF_{SS} is not directly comparable with the RE (A_x) used for the LLGHGs (Fig. 6), and, thus, some manipulations are needed to make them consistent. Since the RF for a sustained emissions is equivalent to the integrated RF of a pulse emissions (see Sect. 3.2), we can estimate the correct RE, A_x, as

$$RF_{ss}(H = 1) = \int_0^1 A_x e^{-\frac{t}{\tau}} = -\tau A_x \left(e^{-\frac{1}{\tau}} - 1 \right) \approx \tau A_x \tag{15}$$

where we assumed $\exp(-1/\tau)$ is negligible since $\tau \gg 1$, hence

$$A_x \approx \frac{RF_{ss}}{\tau} \tag{16}$$

Indirect effects

Chemical Reactions. Emissions of chemically active species can cause changes in concentrations of other species which can have radiative effects. Most relevant in this context are emissions linked to ozone formation or destruction, enhancement of

stratospheric water vapor, changes in concentrations of the OH radical, and secondary aerosol formation. Most indirect effects change the atmospheric residence time of the species (see Sect. 2.1): e.g., CH_4, the ozone-precursors (NO_x, CO, NMVOC), and halocarbons. NO_x also has indirect effects on clouds, see below.

5 *Black Carbon on snow and ice.* For BC, there is an indirect effect of BC deposited on snow and ice as BC reduces the albedo of such surfaces (Warren and Wiscombe, 1980; Jacobson, 2001; Hansen and Nazarenko, 2004; Rypdal et al., 2009; Doherty et al., 2010). The indirect effect of BC on snow and ice raises the impact by 10–15 % (Rypdal et al., 2009; Bond et al., 2011).

10 *Ozone depleting substances*. Chlorine- and bromine-containing halocarbons cause ozone depletion in the stratosphere. While the direct effect of the ODS is warming, they also have a cooling effect via reduction of stratospheric ozone, which may be included in metrics, e.g. GWPs (Daniel et al., 1995).

Contrails and Cirrus. Aviation leads to indirect impacts including formation of con-
15 trails and aviation induced cirrus (AIC). These indirect effects have large uncertainties and their impact will vary greatly due to different flight paths (both horizontally and vertically). The uncertainty on the RF of contrails in the order of 1.5 to 2 and for AIC about an order of 3 (Fuglestvedt et al., 2010).

Aerosol Indirect Effect (AIE). Aerosols have both direct and indirect effects on RF.
20 The direct effects are due to scattering and absorption of radiation, while the indirect effects modify the microphysical and hence the radiative properties, amount and lifetime of clouds. The semi-direct effect includes heating from the aerosols, which result in a cloud burn-off. Aerosols will also impact ice clouds, but the RF from that effect is uncertain. The AIE have usually been split into "cloud albedo effect" (first indirect effect)
25 and the "cloud lifetime effect" (second indirect effect) (Forster et al., 2007). It is difficult to separate which aerosols contribute to the AIE. The indirect effect is almost as large as the direct effect, with a factor of 1.5–2 to account for both effects relative to just the direct effect (Forster et al., 2007).

⏮ | ⏭

◀ | ▶

Back | Close

Full Screen / Esc

Printer-friendly Version

Interactive Discussion

2.3 Regional metric values

For all forcings, even the relatively homogeneous ones caused by LLGHGs, there is a distinct pattern in the temperature response controlled largely by the response pattern of the climate feedbacks (Boer and Yu, 2003; Shindell and Faluvegi, 2009; Shindell, 2012). While the location of emissions does not have an impact on the RF for LL-GHGs, it does for SLCFs (Fuglestvedt et al., 1999; Naik et al., 2005; Berntsen et al., 2006; Shindell and Faluvegi, 2009), leading to a more distinct region distribution of RF (Berntsen et al., 2006; Bond et al., 2011). The heterogeneity in RF causes further inhomogeneity in the climate response pattern to SLCFs.

A schematic presentation of the regional effects is given in Fig. 7 and this is represented mathematically in Eq. (33). Those SLCFs that have an atmospheric residence time of a couple of weeks or less will not have time to be evenly distributed in the global atmosphere and, hence, result in the largest concentration perturbations near the point of emission and its latitude band. In general, strong climate feedbacks at higher latitudes increase the temperature perturbations from RFs, with about 45 % enhancement for extratropical relative to tropical CO_2 RF (Shindell and Faluvegi, 2009). The enhanced regional sensitivities at higher altitudes is a result of the regional energy budget, which is governed by local cloud, water vapor, and surface albedo feedbacks. In addition to variability in physical and chemical key parameters, there are strong nonlinear relations in the atmospheric chemistry.

While most parameterizations of impacts parameters are for global means, recent research has also focused on regional metrics (Lund et al., 2011). Shindell and Faluvegi (2009) separate the world into four latitude bands and estimated regional responses from regional RFs for some selected LLGHGs and SLCFs. This work has been extended by introducing the Absolute Regional Temperature Potential (ARTP) (Shindell, 2012).

2.4 Efficacy

The temperature perturbation from the RF can also depend on the forcing agent, leading to the efficacy, which is defined "as the ratio of the climate sensitivity parameter for a given RF agent (λ_i) to the climate sensitivity parameter for CO_2 changes, that is,

$\varepsilon_i = \lambda i / \lambda_{CO_2}$" (Forster et al., 2007). The efficacy moves one step closer to the actual temperature response by accounting for differences in how various components trigger feedbacks. Efficacies are usually between 0.75 and 1.25 for most components, but more likely 0.5 to 2.0 for aerosol and ozone changes (Forster et al., 2007). Fuglestvedt et al. (2003) proposed, and Berntsen et al. (2005); Berntsen and Fuglestvedt (2008) applied, the efficacy concept to the simple emission metrics.

2.5 Absolute metrics

In the following sections, we present analytical expressions for the different metrics. Emission metrics are obtained by combining the information on the radiative efficiency with IRFs, and, thus, emission metrics only approximate the response of more complex models. However, on the assumption that the emission metrics are applied to marginal emission changes and the metrics are applied to background conditions consistent with the derivation of the metric parameters, these responses should agree to within first-order of the actual response. The largest differences are expected for short-lived species where the location and timing of emissions are important (Lund et al., 2011).

2.5.1 Radiative forcing (RF) as function of t

For emission metrics, the radiative forcing (RF) for all components is calculated as

$$RF = RE \times IRF. \tag{17}$$

In the context of Eq. (1), the impact is RF, and the discount is a Dirac delta function at time t implying an end-point metric. Based on the equations above, the RF for CO_2 is

$$RF_{CO_2}(t) = A_{CO_2}, \left\{ a_0 + \sum_{i=1}^{I} a_i \left(1 - \exp\left(-\frac{t}{\tau_i}\right) \right) \right\} \qquad (18)$$

Further, the equivalent expression for pollutants with a simple exponential decay is

$$RF_x(t) = A_x \exp\left[-\frac{t}{\tau}\right] \qquad (19)$$

The RF for the ozone pre-cursors (OP: NO_x, CO, VOC considered here) is, however, more complex. Due to the short lifetime, it is assumed that the pulse emission lasts one year with constant emissions through the year followed by decay in concentration after end of year 1 (see Sect. 2.2.3) (Fuglestvedt et al., 2010). Hence, the parameterization of RF is split into two parts, the RF that is due the first year of emissions ($t < 1$) and the RF due to the decaying concentration afterwards. The ozone-precursors have an insignificant direct effect on RF; however, there are three indirect effects due to chemical reactions. The short-lived O_3 effect occurs for all the species as a positive RF due to the formation of tropospheric O_3. CO and VOC (NO_x) cause a positive (negative) RF by decreasing (increasing) the OH levels and, thus, increasing (decreasing) the CH_4 levels, which is the methane effect. Since the methane concentration is perturbed, a secondary effect impacts the ozone, called the methane-induced O_3 effect. Hence, CO and VOC (NO_x) will have a positive (negative) RF due to increased (decreased) O_3 caused by the methane perturbation. The perturbations for each of the three effects $RF_{OP}^{O_3}$, $RF_{OP}^{CH_4}$, and $RF_{OP}^{CH_4,PM}$ are

$$RF_{OP}^{S}(t) = \begin{cases} A_{OP}^{S}\left(1 - \exp\left(-\frac{t}{\tau}\right)\right) & 0 < t < 1 \\ A_{OP}^{S}\left(1 - \exp\left(-\frac{1}{\tau}\right)\right)\exp\left(-\frac{t-1}{\tau}\right) & t \geq 1 \end{cases} \qquad (20)$$

890

where OP is the ozone pre-cursors and S is one of the three perturbation effects. The notation differs here from Fuglestvedt et al. (2010). A_{OP}^{S} is the radiative efficiency parameterized as $A_{OP}^{O_3}$, $A_{OP}^{CH_4}$, and $A_{OP}^{CH_4,PM}$ for the short-lived O_3, methane, and methane-induced O_3 perturbation, respectively. The lifetime τ is τ_S for the short-lived O_3 perturbation and τ_{PM} for the methane perturbation and methane-induced O_3 perturbation. This formulation differs slightly from (Fuglestvedt et al., 2010), as they assumed that the very small contribution from the methane-induced O_3 perturbation in year 1 to be included in the short-lived O_3 response, whereas we do not make this assumption. The final RF from the three effects is

$$RF_{OP}(t) = RF_{OP}^{O_3} + RF_{OP}^{CH_4} + RF_{OP}^{CH_4,PM} \tag{21}$$

where OP is either NO_x, CO, or VOC.

2.5.2 Absolute Global Warming Potential (AGWP)

The absolute global warming potential (AGWP) for species i is the integrated RF,

$$AGWP_i(H) = \int_0^H RF_i(t)\,dt \tag{22}$$

In the context of Eq. (1), the impact is RF, with the discounting as a step function (no discounting for $t > H$ and full discounting for $t < H$. Fuglestvedt et al. (2003) estimated an equivalent exponential discount function that gave the same AGWP and found that different species implicitly had different discount rates. The IPCC did not give a direct physical interpretation of the AGWP, but gave some tentative interpretations for three time horizons (20, 100, 500 yr) (IPCC, 1990). They describe that for some environmental impacts it is important to evaluate the cumulative warming over an extended period after the emissions. For instance, the evaluation of sea level rise needs a time horizon

of 100 yr or longer. For short term effects, a time horizon of a few decades could be used, such as the response to RF over continental areas.

The absolute Global Warming Potential (AGWP) for CO_2 is

$$\text{AGWP}_{CO_2}(H) = A_{CO_2}\left\{ a_0 H + \sum_{i=1}^{I} a_i \tau_i \left(1 - \exp\left(-\frac{H}{\tau_i}\right)\right)\right\} \tag{23}$$

and for pollutants with a simple exponential decay

$$\text{AGWP}_x(H) = A_x \tau \left(1 - \exp\left(-\frac{H}{\tau}\right)\right) \tag{24}$$

The formulas are more complex for the ozone pre-cursors (NO_x, CO, VOC), since they have a short-lived O_3 effect ($\text{AGWP}_{OP}^{O_3}$), methane effect ($\text{AGWP}_{OP}^{CH_4}$), and methane-induced O_3 effect ($\text{AGWP}_{OP}^{CH_4,PM}$). Those effects are parameterized as

$$\text{AGWP}_{OP}^{S}(t) = \begin{cases} A_{OP}^S\left\{ H - \tau\left[1 - \exp\left(-\frac{H}{\tau}\right)\right]\right\} & 0 < t < 1 \\ A_{OP}^S\left\{ 1 - \tau\left[\exp\left(-\frac{(H-1)}{\tau}\right) - \exp\left(-\frac{H}{\tau}\right)\right]\right\} & t \geq 1 \end{cases} \tag{25}$$

with different RE A_{OP}^S and lifetime τ for the different perturbations, see Eq. (20). The total effect of the ozone pre-cursor is

$$\text{AGWP}_{OP}(t) = \text{AGWP}_{OP}^{O_3} + \text{AGWP}_{OP}^{CH_4} + \text{AGWP}_{OP}^{CH_4,PM} \tag{26}$$

2.5.3 Absolute Global Temperature change Potential (AGTP)

The absolute global temperature change potential (AGTP) for species i is global temperature change (ΔT) at time t (Shine et al., 2005) is,

$$\text{AGTP}_i(H) = \int_0^t \text{RF}_i(t)\,\text{IRF}_T(H - t)\,\text{d}t, \tag{27}$$

In terms of Eq. (1), the AGTP is generally interpreted as temperature (the whole integral), as an end-point indicator (discounted using a Dirac delta function) with an evaluation time of t. It is also possible to interpret the AGTP with IRF_T as the discount function. A non-zero IRF represents the "discounting" or decay in the surface temperature response caused by the deep ocean (energy is partitioned between the surface ocean, deep ocean, and the share radiated back to space). If $IRF_T = 1$, no discounting, which is the case for AGWP. According to the AGWP, a species with a short (hours, weeks, years) but strong RF will have an impact indefinitely as the integration does not forget this RF; in contrast, the AGTP will "forget" the RF as it is either moves into the deep ocean or is (eventually) radiated back to space (see Peters et al., 2011a).

The absolute Global Temperature Change Potential (AGTP) for CO_2 is

$$\text{AGTP}_{CO_2}(H) = A_{CO_2}\left\{ \sum_{j=1}^{J} a_0 c_j \left[1 - \exp\left(-\frac{H}{d_j}\right) \right] + \sum_{i=1}^{I}\sum_{j=1}^{J} \frac{a_i \tau_i c_j}{\tau_i - d_j}\left[\exp\left(-\frac{H}{\tau_i}\right) - \exp\left(-\frac{H}{d_j}\right) \right] \right\} \quad (28)$$

For pollutants with a simple exponential decay

$$\text{AGTP}_x(H) = \sum_{j=1}^{J} \frac{A_x \tau c_j}{(\tau - d_j)}\left[\exp\left(-\frac{H}{\tau}\right) - \exp\left(-\frac{H}{d_j}\right) \right] \quad (29)$$

The formulas are more complex for the ozone pre-cursors (NO_x, CO, VOC), since they have a short-lived O_3 effect ($\text{AGTP}_{O_3}^{S}$), methane effect (AGTP_{CH_4}), and methane-induced O_3 effect ($\text{AGTP}_{O_3}^{PM}$). For all these effects, there is a perturbation from the RF for $t < 1$ (this determines the temperature response of the emissions that occur in the first year) and from the RF for $t \geq 1$ (this determines the temperature response of atmospheric perturbation lasting past one year). Thus, AGTP_{OP} for $H>1$ is comprised of two components ($\text{AGTP}(H) = \text{AGTP}_{OP}^{S,<1}(H) + \text{AGTP}_{OP}^{S,>1}(H)$):

a. For perturbation from RF occurring $t < 1$

$$\text{AGTP}_{\text{OP}}^{S,<1}(H) = A_{\text{OP}}^S \sum_{j=1}^{J} \left\{ c_j \left[\exp\left(\frac{1-H}{d_j}\right) - \exp\left(-\frac{H}{d_j}\right) \right] \right.$$
$$\left. + \frac{c_j \tau}{\tau - d_j} \left[\exp\left(-\frac{H}{d_j}\right) - \exp\left(\frac{1-H}{d_j}\right) \exp\left(-\frac{1}{\tau}\right) \right] \right\} \tag{30}$$

b. For perturbation from RF occurring $t \geq 1$

$$\text{AGTP}_{\text{OP}}^{S,>1}(H) = A_{\text{OP}}^S \left[1 - \exp\left(-\frac{1}{\tau}\right) \right] \sum_{j=1}^{J} \frac{\tau c_j}{\tau - d_j} \left[\exp\left(\frac{1-H}{\tau}\right) - \exp\left(\frac{1-H}{d_j}\right) \right] \tag{31}$$

The RE A_{OP}^S and lifetime τ differ between the different perturbations, see Eq. (20). These formulas are only valid when $H > 1$, and for continuity it is possible to make a linear interpolation ($aH + b$) between year 0 (where the perturbation is $\text{AGTP}_{\text{OP}}^S(0) = 0$) and year 1. This step is not necessary based on physical processes, but is done to ensure continuity in graphical presentation and for calculating the integrated GTP (next section). For all the three different ozone pre-cursor perturbations, the perturbation for $0 < H < 1$ is given by

$$\text{AGTP}_{\text{OP}}^S(H) = \text{AGTP}_{\text{OP}}^S(1)H, \quad \text{for } 0 < H < 1 \tag{32}$$

It is possible to extend the AGTP into a regional form (cf., Shindell, 2012),

$$\text{ARTP}_i^r(H) = \int_0^t \sum_s \left(\mathbf{K}_i^{rs} \text{RF}_i^s\right) \text{IRF}_T(H - t)\,dt, \tag{33}$$

where r represents the region with the response, s the region of the RF, and $\mathbf{K}^{rs}$ a matrix of scalars relating the RF in s to the response in r, see Fig. 7. A similar

A synthesis of climate-based emission metrics with applications

B. Aamaas et al.

Title Page

Abstract	Introduction
Conclusions	References
Tables	Figures

◄◄ ►►

◄ ►

Back Close

Full Screen / Esc

Printer-friendly Version

Interactive Discussion

expression is possible to link regional emissions with RF, and hence from regional emissions to regional response.

2.5.4 Integrated Absolute Global Temperature change Potential (*i*AGTP)

The integrated temperature change potential (*i*AGTP) for species i is the integral of the AGTP$_i$ (Peters et al., 2011a),

$$i\text{AGTP}_i(H) = \int_0^t \text{AGTP}_i(t)\,dt, \tag{34}$$

In terms of Eq. (1), the impact is temperature, and the discount function is no discounting for $t < H$ and full discounting for $t > H$. The *i*AGTP has been discussed indirectly by some authors (O'Neill, 2000), but in more detail in Peters et al. (2011a). Preliminary work on the GWP was based on integrated temperature change (Wuebbles, 1989; Derwent et al., 1990). The link to temperature, however, did not make it into the First Assessment Report (IPCC, 1990). Peters et al. (2011a) investigated whether the GWP was similar to the *i*GTP and found close agreement for a wide range of time horizons, but not for very SLCFs like BC. The similarity is since AGWP represents the total energy added to the system and *i*AGTP/λ the energy lost from the system. Since the energy currently in the system is small relative to AGWP, it follows that AGWP is approximately *i*AGTP/λ. Given these quantitative relationships, it is arguably better to interpret the AGWP as *i*AGTP.

The integrated absolute Global Temperature Change Potential (*i*AGTP) for CO_2 is (Peters et al., 2011a)

$$i\text{AGTP}_{CO_2} = A^{CO_2} \left\{ \sum_{j=1}^{J} a_0 c_j \left[H - d_j \left(1 - \exp\left(-\frac{H}{d_j} \right) \right) \right] \right.$$
$$\left. + \sum_{i=1}^{I} \sum_{j=1}^{J} \frac{a_i \tau_i c_j}{\tau_i - d_j} \left[\tau_i \left(1 - \exp\left(-\frac{H}{\tau_i} \right) \right) - d_j \left(1 - \exp\left(-\frac{H}{d_j} \right) \right) \right] \right\} \quad (35)$$

While the *i*AGTP for species with a single decay time is

$$i\text{AGTP}_x(H) = \sum_{j=1}^{J} \frac{A_x \tau c_j}{(\tau - d_j)} \left[\tau \left(1 - \exp\left(-\frac{H}{\tau} \right) \right) - d_j \left(1 - \exp\left(-\frac{H}{d_j} \right) \right) \right] \quad (36)$$

For the ozone pre-cursor perturbations, the linear interpolation between year 0 and year 1 for AGTP turns into a quadratic form ($\frac{a}{2} H + b H^2$) for the *i*AGTP. In the range $0 < H < 1$, the perturbation is

$$i\text{AGTP}_{OP}^{S}(H) = \frac{1}{2} \text{AGTP}_{OP}^{S}(1) H^2 \quad (37)$$

This formula is used when $H \leq 1$. For all other times, $i\text{AGTP}_{OP}^{S}(1)$ has to be added into the formula. For $H > 1$, $i\text{AGTP}_{OP}^{S}$ for the short-lived O_3 effect ($i\text{AGTP}_{OP}^{O_3}$), methane effect ($i\text{AGTP}_{OP}^{CH_4}$), and methane-induced O_3 effect ($i\text{AGTP}_{OP}^{O_3,PM}$) have to be summed for the RF from $t < 1$ and for the RF from $t > 1$. Thus, $i\text{AGTP}_{OP}^{S}$ for $H > 1$ is comprised of two components ($i\text{AGTP}(H) = i\text{AGTP}_{OP}^{S,<1}(H) + i\text{AGTP}_{OP}^{S,>1}(H)$):

a. For perturbation from RF occurring $H < 1$

$$i\text{AGTP}_{\text{OP}}^{S,<1}(H) = i\text{AGTP}_{\text{OP}}^{S}(1) + A_{\text{OP}}^{S} \sum_{j=1}^{J} \left\{ c_j d_j \left[1 - \exp\left(\frac{1-H}{d_j}\right) \right. \right.$$
$$\left. + \exp\left(-\frac{H}{d_j}\right) - \exp\left(-\frac{1}{d_j}\right) \right] + \frac{c_j d_j \tau}{\tau - d_j} \left[\exp\left(-\frac{1}{d_j}\right) \right.$$
$$\left. \left. - \exp\left(-\frac{H}{d_j}\right) - \left(1 - \exp\left(\frac{1-H}{d_j}\right)\right) \exp\left(-\frac{1}{\tau}\right) \right] \right\} \tag{38}$$

b. For perturbation from RF occurring $H \geq 1$

$$i\text{AGTP}_{\text{OP}}^{S,>1}(H) = i\text{AGTP}_{\text{OP}}^{S}(1) + A_{\text{OP}}^{S} \left[1 - \exp\left(-\frac{1}{\tau}\right) \right] \sum_{j=1}^{J} \frac{\tau c_j}{\tau - d_j}$$
$$\left[\tau \left(1 - \exp\left(\frac{1-H}{\tau}\right)\right) - d_j \left(1 - \exp\left(\frac{1-H}{d_j}\right)\right) \right] \tag{39}$$

As previously, the RE A_{OP}^{S} and lifetime τ differ between the different perturbations, see Eq. (20).

2.5.5 Other metrics

While the presented metrics are the most used, there is a range of other metrics suitable for different applications. The GWP is the most common emission metric in use, probably since it is used to weight the LLGHGs in the Kyoto Protocol. The AGWP is occasionally used, but often due to its connection with sustained emissions (see below). The AGTP and GTP are the next most common metrics, with both the absolute and normalized forms receiving attention. Other metrics are used, but they are generally

specific to a particular paper or application. In the following we summarize some of the main metrics, but do not go into extensive detail since they are not widely applied.

There are two metrics recently developed which are the same as the iAGTP. For a linear IRF, the "surface temperature response per unit continuous emissions" (STRE) is mathematically equivalent to the iAGTP, though Jacobson (2010) uses a single decay for CO_2 which is inconsistent with the literature (Archer et al., 2009). The Mean Global Temperature change Potential (MGTP) (Gillett and Matthews, 2010) is the iAGTP divided by the TH, and thus in a normalized gas is identical to the iGTP.

Bond et al. (2011) proposed the Specific Forcing Pulse (SFP) that measure the immediate energy perturbation for BC and OC. This metric considers region impacts, because SFP is the amount of energy added to or removed from a receptor region by a chemical species, per mass of emission in a source region. While this metric has only been used for BC and OC, the usage could also extend to other SLCFs with a lifetime significantly less than a year.

Other metrics have been based on economic models. Manne and Richels (2001) investigated how constraints will affect the usage of GWP and impact the pricing of different LLGHGs. Recently, the Global Cost Potential (GCP) and Cost-Effective Temperature Potential (CETP) were developed (Johansson, 2012) which show similar characteristics to the Manne and Richels (2001) study. The time-dependent version of the GTP puts more weight on SLCFs as the target is approached (Shine et al., 2007), a characteristic seen in many economic approaches (Manne and Richels, 2001; Johansson, 2012). This property may be a characteristic of moving towards a target, and not necessarily a characteristic of the economic model. For a cost-benefit framework, the Global Damage Potential (GDP) is suitable, which looks at the marginal damages of emissions (Kandlikar, 1995; Boucher, 2012).

2.6 Normalized metrics

The absolute metrics for a species are often normalized to the corresponding absolute metric for a reference gas, normally CO_2,

$$M_x(t) = \frac{AM_x(t)}{AM_{CO_2}(t)} \qquad (40)$$

where AM stands for AGWP, AGTP, or iAGTP and M is GWP, GTP, or iGTP, respectively. Emissions E_x are usually be converted into so called f "CO_2 equivalent emissions" by multiplying with this normalized metric,

$$CO_2eq(t) = M_x(t) \times E_x \qquad (41)$$

that would ideally results in the same climate response for the given metric; e.g. for GWP100 there is equivalence in RF integrated up to 100 yr and for GTP the same temperature change for the chosen year (Fuglestvedt et al., 2003; O'Neill, 2000). But this equivalence is not present for other climate variables beyond what the metric measures. The GWP is the most common emission metric in use, and is used to weight the LLGHG in the Kyoto Protocol. The AGWP is occasionally used, but often due to its connection with sustained emissions (see below). The AGTP and GTP are the next most common metrics, with both the absolute and normalized forms receiving attention.

In terms of weighting GHGs, a time-dependent version of the GTP has been developed, GTP(TE – t), where TE represents the year a temperature target is specified (e.g., 2 degree limit in 2100). The time-dependency puts more relative weight on SLCFs as the target is approached, a characteristic seen in many economic approaches (Manne and Richels, 2001; Johansson, 2012). This property may be a characteristic of moving towards a target, and not necessarily a characteristic of the economic model. The iAGTP and iGTP is a relatively new metric (Peters et al., 2011a), with applications so far mainly in the interpretation of the AGWP and GWP.

The normalized metric is dependent on the absolute metric of CO_2, since the absolute metric of CO_2 is the denominator. We show the importance of the denominator in the case of CH_4 for GWP in Fig. 8. For time horizons (H) less or around a species' lifetime (τ), GWP is affected by AGWP for both the species and CO_2, as both AGWPs are sensitive of time horizon. However, as time horizon increases, the changes in the GWP depend only on the changes in AGWP for CO_2 since the AGWP for CH_4 converges to its steady-state value soon after the lifetime (dependent on the e-folding time). The same is true for all SLCFs, where species reach this threshold increasingly faster with decreasing lifetimes. Hence, for $\tau \gg H$, the changes in the GWP value of a species depends only on the behavior of CO_2 (e.g., BC the order of months, or CH_4 the order of decades).

3 Methods for scenarios and sustained emissions

The response of a pulse emission can be seen as the building block of the response from an emission scenario via convolutions (Enting, 2007; Wigley, 1991). Pulse emissions are used due to their simplicity and generality and are, thus, preferred by the science community. On the other hand, policy makers may have greater interest in the comparison of emission scenarios. A pulse emission is also a type of scenario, where emissions are assumed to stop instantaneously. A particularly type of scenario often used in emission metrics is a sustained emission which assumes emissions continue indefinitely at a pre-defined level. While SLCFs are quickly forgotten in the response of a pulse emission, both the impacts of SLCFs and the LLGHGs are present in a sustained emission scenario. It is also possible to have more general emissions scenarios (Moss et al., 2010), though these are not often used as for emission metrics, but are used to compare the response over time (such as the temperature response to a given scenario). We will first present the simplest emission scenario, sustained emissions, followed by the more general case. We also expand on the relationship between pulse and sustained emission metrics.

A synthesis of climate-based emission metrics with applications

B. Aamaas et al.

Title Page

Abstract | Introduction

Conclusions | References

Tables | Figures

◄ | ►

◄ | ►

Back | Close

Full Screen / Esc

Printer-friendly Version

Interactive Discussion

3.1 Sustained emissions

A simple emission scenario is to have a continuation of the pulse emissions, which are sustained emissions. The absolute metric of a sustained emission can be calculated as the integral of the absolute metric of a pulse emission (see Sect. 3.2). Sustained emissions are a specific type of scenario that neglects changes due to economic growth, technology improvements, mitigation policies or the lifecycle of infrastructure. From a policy perspective, sustained emission may be more relevant, since in reality, emissions are unlikely to stop instantaneously as in a pulse emission. However, from a scientific perspective, processes easily observable in a pulse emission can be masked by a sustained emission. The choice between a pulse and sustained emission scenario is an important value judgment as they place very different weights on SLCFs and LLGHGs.

In the following, we show the equations for the different metrics with sustained emissions. The RF for species with a simple exponential decay and sustained emission is

$$\text{RF}_{x,\text{s}}(H) = A_x \tau \left(1 - \exp\left(-\frac{H}{\tau} \right) \right) \tag{42}$$

This equation is identical to the AGWP for a pulse emission, and this point is returned to in the following section. The AGWP for a sustained emission is

$$\text{AGWP}_{x,\text{s}}(H) = A_x \tau \left[H - \tau \left(1 - \exp\left(-\frac{H}{\tau} \right) \right) \right] \tag{43}$$

The AGTP for a sustained emission is

$$\text{AGTP}_{x,\text{s}}(H) = \sum_{j=1}^{J} A_x \tau \lambda \left(1 - \exp\left(-\frac{H}{d_j} \right) \right) + \text{AGTP}_x(H) \tag{44}$$

And finally, the iAGTP for a sustained emission is

$$i\text{AGTP}_{x,\text{s}}(H) = \sum_{j=1}^{J} A_x \tau \lambda \left(H - d_j \left(1 - \exp\left(-\frac{H}{d_j}\right)\right)\right) + i\text{AGTP}_x(H) \tag{45}$$

Similar equations can be derived for CO_2 and ozone precursors, but are not shown here in the interests of space.

3.2 Connecting pulse and sustained emission metrics

A property of convolutions with a linear response and the Heaviside step function (equivalent to a sustained emission), leads to the RF of a sustained emission (RF_s, left hand side) is equal to the integrated RF of a pulse emission (AGWP, right hand side),

$$\text{RF}_{x,\text{s}}(t) = \int_0^t H(s) R_x(t-s)\,\text{d}s = \int_0^t R_x(s)\,ds = \int_0^t \text{RF}_{x,p}(s)\,\text{d}s = \text{AGWP}_x(t) \tag{46}$$

Further, the same is true for a linear temperature response,

$$\Delta T_{x,\text{s}}(t) = \int_0^t \text{RF}_{x,\text{s}}(s) R_T(t-s)\,\text{d}s = \int_0^t \text{AGWP}_x(s) R_T(t-s)\,\text{d}s = i\text{AGTP}_x(t) \tag{47}$$

so that the instantaneous temperature perturbation to a sustained emission is equal to the integrated temperature perturbation to a pulse emission. Thus, there is a close connection between pulse and sustained emission metrics; the instantaneous impact of a sustained emission is the same as the integrated impact of a pulse emission. In early work, Shine et al. (2005) noted that the GWP was similar to the instantaneous temperature response to a sustained emission. This is equivalent to the integrated temperature response of a pulse emissions, and this has been shown to be similar to the GWP (Peters et al., 2011a), thus, confirming the findings of Shine et al. (2005).

3.3 Convolution

For emission scenarios, the RF, AGWP, AGTP, and iAGTP values can be calculated with a convolution,

$$(f \times g)(t) = \int_{-\infty}^{\infty} f(s)\, g(t-s)\, \mathrm{d}s \tag{48}$$

where f and g are functions and g represents the emission metric for a pulse emission. For instance, the AGTP for a scenario is the convolution of the emission scenario and AGTP for a pulse emission:

$$\mathrm{AGTP}_i^{\mathrm{Scenario}}(t) = \int_0^t E_i(\tau)\, \mathrm{AGTP}_i^{\mathrm{Pulse}}(t-\tau)\, \mathrm{d}\tau \tag{49}$$

Thus, the AGTP is an IRF representing the link from emissions to temperature (IRF_T is the link from forcing to temperature). The convolution can be estimated by numerical integration, such as with a simple summation, using the Trapezoidal rule, Simpson's rule, numerical quadrature and so on. Most numerical integrations have problems with species with a short lifetime (e.g. BC), typically when the time step is larger than the residence time ($\Delta t > \tau$). This problem can be solved by reducing the time step; however, this greatly slows down the calculation time.

If the IRF is based on a sum of exponentials, then the convolution can be written as an equivalent ordinary differential equation (ODE) (Wigley, 1991).

$$\frac{\mathrm{d}F(H)}{\mathrm{d}t} = \sum_{k=1}^{K} \frac{\mathrm{d}F_k(H)}{\mathrm{d}t} = E(H) \sum_{k=1}^{K} \alpha_k - \sum_{k=1}^{K} \frac{F_k}{\tau_k} \tag{50}$$

The ODE can be solved numerically and we find this to be a more robust and efficient method than the direct estimation of the convolution numerically. This method requires

a response based on exponential functions, and thus cannot be applied directly to emission metrics as in Eq. (49). However, a step-wise series of convolutions and integrations can perform the necessary calculations; the RF can be determined using this method with integration leading to the integrated RF, another convolution with IRF_T leading to temperature, and integration leading to integrated temperature.

4 Sample applications

In this section, we present some more specific and policy relevant applications using the emission metrics described above. Since climate metrics are based on simple parameterizations of more complex models (e.g., the Hadley CM3 is reduced to four parameters), then it is expected that metric values only approximate the actual responses. However, the estimated responses should capture the key first-order effects and, hence, not deviate substantially from the likely temperature response. As input data, we used the 2008 emissions from the Emissions Database for Global Atmospheric Research (EDGAR) (EC, 2011), with the exception of BC and OC from 2005 (Zbigniew Klimont, personal communication, 2012). The IRF for CO_2 is based on the Bern Carbon Cycle Model (Joos et al., 2001) as reported in Forster et al. (2007), and a recent model intercomparison shows that the Bern model is likely to be close to the model mean (Joos et al., 2012). The IRF for temperature is based on the Hadley CM3 climate model (Boucher and Reddy, 2008), and a recent model comparison (Olivié and Peters, 2012) shows the magnitude of the model spreads. The remaining RE and lifetimes for the long-lived greenhouse gases are from Forster et al. (2007), for BC, OC, direct SO_2, contrail, and aircraft induced cirrus from Fuglestvedt et al. (2010). The parameters for aircraft NO_x are from Stevenson et al. (2004), for surface NO_x the global run from Wild et al. (2001), for CO the mean of UiO and LMDz runs from Berntsen et al. (2005), and for VOC from Collins et al. (2002), as given by Fuglestvedt et al. (2010). NH_3 is based on Shindell et al. (2009). The BC parameterization here does not consider the impact of BC in snow.

The AIE is normally applied in the metrics by scaling it relative to the direct aerosol effect. The scaling is obtained using globally averaged values and is crudely set to 1.5–2, with the direct aerosol effect and indirect aerosol effect have radiative forcings of about $-0.5\,\mathrm{W\,m^{-2}}$ and $-0.4\,\mathrm{W\,m^{-2}}$, respectively (Forster et al., 2007). However, many different aerosols can lead to the AIE, and it is currently poorly understood which aerosols, or mix of aerosols, lead to the AIE. Our default case is to assume the AIE is entirely due to SO_2. With that assumption, we can scale AIE in shipping as the indirect effect of SO_2 given by the average of Lauer et al. (2007), which scales AIE to be 830 % of the direct effect. For all other sectors, the AIE can be estimated to be about 75 % of the direct effect of SO_2 (Forster et al., 2007). If we didn't scale shipping by 830 %, then, the AIE would be 75 % of the direct effect. We have also tested a variety of other cases to see how the AIE may vary if it is due to a mix of aerosols. In one case, we based the AIE on a mix of BC 10 %, OC 30 %, and SO_2 60 %. Hence, we have tested the robustness of the ranking given the ranges for AIE. The ranking of sectors for global emissions differs little between the parameterizations, and these small variations are only observed for the shortest time horizons.

4.1 Metric values as a function of time-horizon

The GWP, GTP, and iGTP values for a range of pollutants are shown in Fig. 9 based on equations in Sects. 2.5.2, 2.5.3, and 2.5.4. Since both GWP and iGTP integrate the effects over time, both these metrics "remember" what occurred previously, even though for a pulse emissions the RF eventually decays to zero as energy is radiated back to space. GTP is an end-point metric that only looks at the climate system at a specific time. As shown in earlier work, there is a similarity between the GWP and iGTP, but neither is similar to the GTP (Peters et al., 2011a). The GTP values are generally lower. Organic carbon (OC) and SO_2 have negative RF and, hence, negative metric values for all times. Some of the ozone precursors (NO_x, CO, VOC) are initially negative (positive) and, then, change sign as different responses take effect. Almost all species become less important with time relative to CO_2, with the exception of N_2O.

For N_2O, it takes about 50 yr before its GTP value begins to decrease. In general, the climate impact is governed by species with strong, but short-lived impact and weak, but long-lived impacts.

It is also possible to have metrics with a variable time horizon, where the target year (TY) is fixed and the time horizon is reduced as the target year is approaching, $TH(t) = TY - t$ (Shine et al., 2007). Metrics with such a variable time horizon can be visualized as the mirror image of Fig. 9 (along the time-horizon axis). As the target year is approached, the importance of the SLCFs increases. For the LLGHGs, the metric values are rather constant throughout the period.

4.2 Ranking of countries with different metrics

Figure 10 shows the CO_2-equivalent emissions for global emissions, including both SLCFs and LLGHGs and using different emission metrics. The emissions are the estimates for 2008 from EDGAR, with the exception of BC and OC for 2005. The importance of the SLCFs decreases with increasing time horizon and have little relative weight according to GTP with a 100 yr time horizon. CO_2 dominates the metric weighted emissions in all cases, even when GTP20 is used. In Table 3, we rank countries according to climate impact by using different emission metrics. For the top five emitters, their ranking does not change with the use of different emission metrics, with the exception of GWP20, since CO_2 emissions dominate the total climate response; however, their relative share of global emissions differs. For instance, China's share of global emissions varies between 14.1 % and 20.9 % using the GWP20 and GTP100. The ranking based on GWP20 differs since the impact of SLCFs is largest for this metric, for instance the cooling from SO_2 is significant for that metric and SO_2 emissions vary between countries. For the countries not in the top-5, rankings are similar with different metrics and changes in the rankings only occur if two countries have similar total emissions.

Within each country, the relative weights of SLCFs and LLGHGs can changes significantly with different metrics. Table 4 shows the relative share of methane in the total

emissions using different emission metrics for the top ten emitters. The share attributed to methane decreases with time horizon, as methane has a much shorter response time than CO_2. Many developing countries have relative large methane emissions and are particularly affected by changing metrics. Using a GWP100, methane represents about 34 % of the total emissions in Brazil and India, but this increases to about 54 % and 55 % with GTP20. China and the Russian Federation have 23 % and 26 % allocated to methane for a GWP100, but increasing to 42 % and 45 % with GTP20. Thus, changing emission metric may have a significant impact on the distribution of emissions allocated to each country, and consequently, this may have significant effects on mitigation costs.

4.3 Metrics and ΔT by source, sector, and component

Figure 11 shows the estimated temperature perturbation based on time dependent AGTP as calculated by Eq. (48) for pulse and sustained emissions of EDGAR year 2008 according to species for China, the USA, and globally. While the SLCFs are important for the temperature perturbation in the first years after a pulse emission, CO_2 dominates in the long run, which is due to longer response time for CO_2 than most other species. In the sustained emission case, the emissions continue into the atmosphere indefinitely; hence, the temperature perturbation from SLCFs is not reduced as time increases, but instead reaches approximately steady-state. However, the concentration of CO_2 increases with time as it does not decay to zero and, thus, accumulates in the atmosphere, leading to a near linear increase in the temperature perturbation from CO_2 emissions. The differences between countries are rather small. After 100 yr of 2008 emissions, the global temperature will have risen by 2.3 °C.

The same estimated temperature perturbation is divided according to sectors in Fig. 12. Instantaneous pulse emissions for 2008 emissions from all sectors give rise to warming, with the exception of cooling from the power and industry sectors in the first 5–20 yr and a small cooling from shipping in the first 40 yr. The cooling is due to emissions of SO_2 and is more persistent in China due to the higher emissions of SO_2

Title Page

Abstract | Introduction

Conclusions | References

Tables | Figures

◄◄ | ►►

◄ | ►

Back | Close

Full Screen / Esc

Printer-friendly Version

Interactive Discussion

relative to CO_2. If we exclude the AIE, the cooling occurs only in the first 5 yr for the power and industry sectors and between year 10 and 30 for shipping. In the long run, the power and industry sectors have the largest perturbation for both pulse and sustained emissions, as CO_2 dominates over the cooling components. Only the shipping sector has a continuous negative contribution in the sustained case; however, note that this assumes no changes in technology into the future.

While Figs. 11 and 12 consider emissions by species and sector separately as a function of time; Fig. 13 shows the contribution of the different sectors by species after 50 yr for China, USA, EU, and the World. Globally, the largest sectors according to AGTP50 are power, industry, biomass burning, and on-road transportation. CO_2 has overall the largest impact, while CH_4 dominates the sectors animal husbandry and waste and N_2O dominates agriculture. Emissions of synthetic gases come mainly from the industry sector.

5 Conclusions

We have presented the parameterizations and analytical expressions of radiative forcing, integrated radiative forcing, temperature, and integrated temperature in both absolute and normalized forms for three types of species: species with a simple exponential decay, CO_2 which has a complex decay over time, and ozone pre-cursors (NO_x, CO, VOC). Since the purpose of using metrics differs, different metrics and time horizons may be preferable for different applications. We have discussed key issues and assumptions in the various parameterizations, particularly in relation to deriving Impulse Response Functions, radiative efficiencies, lifetimes, and a range of indirect effects. Finally, we applied the metrics in a variety of different applications to show their utility, particularly in getting policy relevant information without the need for detailed GCM simulations. The sample applications show that CO_2 is important regardless of what metric and time horizon is used, but that the importance of SLCFs varies greatly depending

References

Archer, D. and Brovkin, V.: The millennial atmospheric lifetime of anthropogenic CO_2, Climatic Change, 90, 283–297, doi:10.1007/s10584-008-9413-1, 2008.

Archer, D., Eby, M., Brovkin, V., Ridgwell, A., Cao, L., Mikolajewicz, U., Caldeira, K., Matsumoto, K., Munhoven, G., Montenegro, A., and Tokos, K.: Atmospheric lifetime of fossil fuel carbon dioxide, Annu. Rev. Earth Pl. Sc., 37, 117–134, 2009.

Berntsen, T. and Fuglestvedt, J. S.: Global temperature responses to current emissions from the transport sectors, P. Natl. Acad. Sci., 105, 19154–19159, doi:10.1073/pnas.0804844105, 2008.

Berntsen, T., Fuglestvedt, J. S., Joshi, M., Shine, K., Stuber, N., Li, L., Hauglustaine, D., and Ponater, M.: Climate response to regional emissions of ozone precursers: Sensitivities and warming potentials, Tellus B, 57, 283–304, 2005.

Berntsen, T., Fuglestvedt, J. S., Myhre, G., Stordal, F., and Berglen, T. F.: Abatement of greenhouse gases: Does location matter?, Climatic Change, 74, 377–411, 2006.

Boer, G. B. and Yu, B. Y.: Climate sensitivity and response, Clim. Dynam., 20, 415–429, doi:10.1007/s00382-002-0283-3, 2003.

Bond, T. C., Zarzycki, C., Flanner, M. G., and Koch, D. M.: Quantifying immediate radiative forcing by black carbon and organic matter with the Specific Forcing Pulse, Atmos. Chem. Phys., 11, 1505–1525, doi:10.5194/acp-11-1505-2011, 2011.

Boucher, O.: Comparison of physically- and economically-based CO_2-equivalences for methane, Earth Syst. Dynam., 3, 49–61, doi:10.5194/esd-3-49-2012, 2012.

Boucher, O. and Reddy, M. S.: Climate trade-off between black carbon and carbon dioxide emissions, Energ. Policy, 36, 193–200, 2008.

5 Boucher, O., Friedlingstein, P., Collins, B., and Shine, K. P.: The indirect global warming potential and global temperature change potential due to methane oxidation, Environ. Res. Lett., 4, 044007, doi:10.1088/1748-9326/4/4/044007, 2009.

Caldeira, K. and Kasting, J. F.: Insensitivity of global warming potentials to carbon dioxide emission scenarios, Nature, 366, 251–253, 1993.

10 Collins, W. J., Derwent, R. G., Johnson, C. E., and Stevenson, D. S.: The oxidation of organic compounds in the troposphere and their global warming potentials, Climatic Change, 52, 453–479, doi:10.1023/a:1014221225434, 2002.

Collins, W. J., Sitch, S., and Boucher, O.: How vegetation impacts affect climate metrics for ozone precursors, J. Geophys. Res., 115, D23308, doi:10.1029/2010jd014187, 2010.

15 Daniel, J. S., Solomon, S., and Albritton, D. L.: On the evaluation of halocarbon radiative forcing and global warming potentials, J. Geophys. Res., 100, 1271–1285, doi:10.1029/94jd02516, 1995.

Derwent, R. G., Environmental, U. K. A. E. A., and Division, M. S.: Trace gases and their relative contribution to the greenhouse effect, AEA Technology, Atomic Energy Research

20 Establishment, 1990.

Doherty, S. J., Warren, S. G., Grenfell, T. C., Clarke, A. D., and Brandt, R. E.: Light-absorbing impurities in Arctic snow, Atmos. Chem. Phys., 10, 11647–11680, doi:10.5194/acp-10-11647-2010, 2010.

Eby, M., Zickfeld, K., Montenegro, A., Archer, D., Meissner, K. J., and Weaver, A. J.: Lifetime of

25 anthropogenic climate change: Millennial time scales of potential CO_2 and surface temperature perturbations, J. Climate, 22, 2501–2511, doi:10.1175/2008jcli2554.1, 2009.

EC: Emission database for global atmospheric research (edgar), release version 4.2., edited by: European Commission, J. R. C. J. N. E. A. A. P., available at: http://edgar.jrc.ec.europa.eu/ (last access: 19 July 2012), 2011.

30 Enting, I. G.: Laplace transform analysis of the carbon cycle, Environ. Modell. Softw., 22, 1488–1497, doi:10.1016/j.envsoft.2006.06.018, 2007.

Title Page

Abstract   Introduction

Conclusions   References

Tables   Figures

◄   ►

◄   ►

Back   Close

Full Screen / Esc

Printer-friendly Version

Interactive Discussion

Enting, I. G., Wigley, T. M. L., and Heimann, M.: Future emissions and concentrations of carbon dioxide: Key ocean/atmosphere/land analyses, CSIRO Division of Atmospheric Research Technical Paper no. 31, 1994.

Forster, P., Ramaswamy, V., Artaxo, P., Berntsen, T., Betts, R., Fahey, D. W., Haywood, J., Lean, J., Lowe, D. C., Myhre, G., Nganga, J., Prinn, R., Raga, G., Schulz, M., and Dorland, R. V.: Changes in atmospheric constituents and in radiative forcing, in: Climate change 2007: The physical science basis. Contribution of working group i to the fourth assessment report of the intergovernmental panel on climate change, edited by: Solomon, S., Qin, D., Manning, M., Chen, Z., Marquis, M., Averyt, K. B., Tignor, M., and Miller, H. L., Cambridge University Press, Cambridge, United Kingdom and New York, NY, USA, 2007.

Friedlingstein, P., Cox, P., Betts, R., Bopp, L., von Bloh, W., Brovkin, V., Cadule, P., Doney, S., Eby, M., Fung, I., Bala, G., John, J., Jones, C., Joos, F., Kato, T., Kawamiya, M., Knorr, W., Lindsay, K., Matthews, H. D., Raddatz, T., Rayner, P., Reick, C., Roeckner, E., Schnitzler, K. G., Schnur, R., Strassmann, K., Weaver, A. J., Yoshikawa, C., and Zeng, N.: Climate–carbon cycle feedback analysis: Results from the c4mip model intercomparison, J. Climate, 19, 3337–3353, doi:10.1175/jcli3800.1, 2006.

Fuglestvedt, J. S., Berntsen, T., Myhre, G., Rypdal, K., and Skeie, R. B.: Climate forcing from the transport sectors, P. Natl. Acad. Sci., 105, 454–458, doi:10.1073/pnas.0702958104, 2008.

Fuglestvedt, J. S., Berntsen, T. K., Isaksen, I. S. A., Mao, H., Liang, X.-Z., and Wang, W.-C.: Climatic forcing of nitrogen oxides through changes in tropospheric ozone and methane; global 3D model studies, Atmos. Environ., 33, 961–977, doi:10.1016/s1352-2310(98)00217-9, 1999.

Fuglestvedt, J. S., Berntsen, T., Godal, O., and Skovdin, T.: Climate implications of gwp-based reductions in greenhouse gas emissions, Geophys. Res. Lett., 27, 409–412, 2000.

Fuglestvedt, J. S., Berntsen, T. K., Godal, O., Sausen, R., Shine, K. P., and Skodvin, T.: Metrics of climate change: Assessing radiative forcing and emission indices, Climatic Change, 58, 267–331, 2003.

Fuglestvedt, J. S., Shine, K. P., Berntsen, T., Cook, J., Lee, D. S., Stenke, A., Skeie, R. B., Velders, G. J. M., and Waitz, I. A.: Transport impacts on atmosphere and climate: Metrics, Atmos. Environ., 44, 4648–4677, 2010.

Gillett, N. P. and Matthews, H. D.: Accounting for carbon cycle feedbacks in a comparison of the global warming effects of greenhouse gases, Environ. Res. Lett., 5, 034011, doi:10.1088/1748-9326/5/3/034011, 2010.

Title Page

Abstract | Introduction

Conclusions | References

Tables | Figures

◀◀ | ▶▶

◀ | ▶

Back | Close

Full Screen / Esc

Printer-friendly Version

Interactive Discussion

Hansen, J. and Nazarenko, L.: Soot climate forcing via snow and ice albedos, P. Natl. Acad. Sci. USA, 101, 423–428, doi:10.1073/pnas.2237157100, 2004.

Hansen, J., Sato, M., Ruedy, R., Nazarenko, L., Lacis, A., Schmidt, G. A., Russell, G., Aleinov, I., Bauer, M., Bauer, S., Bell, N., Cairns, B., Canuto, V., Chandler, M., Cheng, Y., Del Genio, A., Faluvegi, G., Fleming, E., Friend, A., Hall, T., Jackman, C., Kelley, M., Kiang, N., Koch, D., Lean, J., Lerner, J., Lo, K., Menon, S., Miller, R., Minnis, P., Novakov, T., Oinas, V., Perlwitz, J., Perlwitz, J., Rind, D., Romanou, A., Shindell, D., Stone, P., Sun, S., Tausnev, N., Thresher, D., Wielicki, B., Wong, T., Yao, M., and Zhang, S.: Efficacy of climate forcings, J. Geophys. Res., 110, D18104, doi:10.1029/2005jd005776, 2005.

Hodnebrog, Ø., Etminan, M., Fuglestvedt, J. S., Marston, G., Myhre, G., Nielsen, C. J., Shine, K. P., and Wallington, T. J.: Global warming potentials and radiative efficiencies of halocarbons and related compounds: A comprehensive review, Rev. Geophys., submitted, 2012.

Huijbregts, M. A. J., Hellweg, S., and Hertwich, E.: Do we need a paradigm shift in life cycle impact assessment?, Environ. Sci. Technol., 45, 3833–3834, doi:10.1021/es200918b, 2011.

IPCC: Climate change: The ipcc scientific assessment, edited by: Houghton, J. T., Jenkins, G. J., and Ephraums, J. J., Ephraums, Cambridge University Press, Cambridge, United Kingdom, 1990.

IPCC: Radiative forcing of climate change and an evaluation of the IPCC IS92 emission scenarios, edited by: Houghton, J. T., Filho, L. G. M., Bruce, J., Lee, H., Callander, B. A., Haites, E., Harris, N., and Maskell, K., Cambridge University Press, United Kingdom, 1994.

IPCC: The science of climate change, edited by: Houghton, J. T., Meira Filho, L. G., Callender, B. A., Harris, N., Kattenberg, A., and Maskell, K., Cambridge University Press, Cambridge, United Kingdom, 1995.

IPCC: Climate change 2001 – the scientific basis, Cambridge University Press, Cambridge, UK, 2001.

IPCC: Climate change 2007: The physical science basis. Contribution of working group i to the fourth assessment report of the intergovernmental panel on climate change, edited by: Solomon, S., Qin, D., Manning, M., Chen, Z., Marquis, M., Averyt, K. B., Tignor, M., and Miller, H. L., Cambridge University Press, Cambridge, United Kingdom and New York, NY, USA, 2007.

Isaksen, I. S. A., Ramaswamy, V., Rodhe, H., and Wigley, T. M. L.: Radiative forcing of climate change, in: Climate change 1992: The supplementary report to the ipcc scientific assessment, Cambridge University Press, Carmbridge, 47–68, 1992.

Jacobson, M. Z.: Strong radiative heating due to the mixing state of black carbon in atmospheric aerosols, Nature, 409, 695–697, 2001.

Jacobson, M. Z.: Short-term effects of controlling fossil-fuel soot, biofuel soot and gases, and methane on climate, arctic ice, and air pollution health, J. Geophys. Res., 115, D14209, doi:10.1029/2009jd013795, 2010.

Johansson, D.: Economics- and physical-based metrics for comparing greenhouse gases, Climatic Change, 110, 123–141, doi:10.1007/s10584-011-0072-2, 2012.

Joos, F., Bruno, M., Fink, R., Siegenthaler, U., Stocker, T. F., Le QuéRé, C., and Sarmiento, J. L.: An efficient and accurate representation of complex oceanic and biospheric models of anthropogenic carbon uptake, Tellus B, 48, 397–417, doi:10.1034/j.1600-0889.1996.t01-2-00006.x, 1996.

Joos, F., Prentice, I. C., Sitch, S., Meyer, R., Hooss, G., Plattner, G.-K., Gerber, S., and Hasselmann, K.: Global warming feedbacks on terrestrial carbon uptake under the intergovernmental panel on climate change (IPCC) emission scenarios, Global Biogeochem. Cy., 15, 891–907, doi:10.1029/2000gb001375, 2001.

Joos, F., Roth, R., Fuglestvedt, J. S., Peters, G. P., Enting, I. G., von Bloh, W., Brovkin, V., Burke, E. J., Eby, M., Edwards, N. R., Friedrich, T., Frölicher, T. L., Halloran, P. R., Holden, P. B., Jones, C., Kleinen, T., Mackenzie, F., Matsumoto, K., Meinshausen, M., Plattner, G.-K., Reisinger, A., Segschneider, J., Shaffer, G., Steinacher, M., Strassmann, K., Tanaka, K., Timmermann, A., and Weaver, A. J.: Carbon dioxide and climate impulse response functions for the computation of greenhouse gas metrics: a multi-model analysis, Atmos. Chem. Phys. Discuss., 12, 19799–19869, doi:10.5194/acpd-12-19799-2012, 2012.

Kandlikar, M.: The relative role of trace gas emissions in greenhouse abatement policies, Energ. Policy, 23, 879–883, doi:10.1016/0301-4215(95)00108-u, 1995.

Kandlikar, M.: Indices for comparing greenhouse gas emissions: Integrating science and economics, Energy Econ., 18, 265–281, 1996.

Lashof, D. A. and Ahuja, D. R.: Relative contributions of greenhouse gas emissions to global warming, Nature, 344, 529–531, 1990.

Lauer, A., Eyring, V., Hendricks, J., Jöckel, P., and Lohmann, U.: Global model simulations of the impact of ocean-going ships on aerosols, clouds, and the radiation budget, Atmos. Chem. Phys., 7, 5061–5079, doi:10.5194/acp-7-5061-2007, 2007.

Lelieveld, J. and Crutzen, P. J.: Indirect chemical effects of methane on climate warming, Nature, 355, 339–342, 1992.

Title Page

Abstract | Introduction

Conclusions | References

Tables | Figures

◄◄ | ►►

◄ | ►

Back | Close

Full Screen / Esc

Printer-friendly Version

Interactive Discussion

Li, S. and Jarvis, A.: Long run surface temperature dynamics of an a-ogcm: The hadcm3 $4\times CO_2$ forcing experiment revisited, Clim. Dynam., 33, 817–825, doi:10.1007/s00382-009-0581-0, 2009.

Li, S., Jarvis, A. J., and Leedal, D. T.: Are response function representations of the global carbon cycle ever interpretable?, Tellus B, 61, 361–371, doi:10.1111/j.1600-0889.2008.00401.x, 2009.

Lund, M., Berntsen, T., Fuglestvedt, J., Ponater, M., and Shine, K.: How much information is lost by using global-mean climate metrics? An example using the transport sector, Climatic Change, 113, 1–15, doi:10.1007/s10584-011-0391-3, 2011.

Manne, A. S. and Richels, R. G.: An alternative approach to establishing trade-offs among greenhouse gases, Nature, 410, 675–677, 2001.

Manning, M. and Reisinger, A.: Broader perspectives for comparing different greenhouse gases, P. R. Soc. A, 369, 1891–1905, 2011.

Moss, R. H., Edmonds, J. A., Hibbard, K. A., Manning, M. R., Rose, S. K., van Vuuren, D. P., Carter, T. R., Emori, S., Kainuma, M., Kram, T., Meehl, G. A., Mitchell, J. F. B., Nakicenovic, N., Riahi, K., Smith, S. J., Stouffer, R. J., Thomson, A. M., Weyant, J. P., and Wilbanks, T. J.: The next generation of scenarios for climate change research and assessment, Nature, 463, 747–756, 2010.

Myhre, G., Highwood, E., Shine, K. P., and Stordal, F.: New estimates of radiative forcing due to well mixed greenhouse gases, Geophys. Res. Lett., 25, 2715–2718, 1998.

Naik, V., Mauzerall, D., Horowitz, L., Schwarzkopf, M. D., Ramaswamy, V., and Oppenheimer, M.: Net radiative forcing due to changes in regional emissions of tropospheric ozone precursors, J. Geophys. Res., 110, D24306, doi:10.1029/2005jd005908, 2005.

O'Neill, B. C.: The jury is still out on global warming potentials, Climatic Change, 44, 427–443, doi:10.1023/a:1005582929198, 2000.

Olivié, D. J. L. and Peters, G.: The impact of model variation in CO_2 and temperature impulse response functions on emission metrics, Earth Syst. Dynam. Discuss., in press, 2012.

Olivié, D. J. L., Peters, G., and Saint-Martin, D.: Atmosphere response time scales estimated from AOGCM experiments, J. Climate, online first: doi:10.1175/JCLI-D-11-00475.1, 2012.

Pennington, D. W., Potting, J., Finnveden, G., Lindeijer, E., Jolliet, O., Rydberg, T., and Rebitzer, G.: Life cycle assessment Part 2: Current impact assessment practice, Environ. Int., 30, 721–739, 2004.

Title Page

Abstract | Introduction

Conclusions | References

Tables | Figures

◄ | ►|

◄ | ►

Back | Close

Full Screen / Esc

Printer-friendly Version

Interactive Discussion

Peters, G. P., Aamaas, B., Berntsen, T., and Fuglestvedt, F. S.: The integrated global temperature change potential (igtp) and relationship with other simple emission metrics, Environ. Res. Lett., 6, 044021, doi:10.1088/1748-9326/6/4/044021, 2011a.

Peters, G. P., Aamaas, B., Lund, M. T., Solli, C., and Fuglestvedt, J. S.: Alternative "global warming" metrics in life cycle assessment: A case study with existing transportation data, Environ. Sci. Technol., 45, 8633–8641, doi:10.1021/es200627s, 2011b.

Pinnock, S., Hurley, M. D., Shine, K. P., Wallington, T. J., and Smyth, T. J.: Radiative forcing of climate by hydrochlorofluorocarbons and hydrofluorocarbons, J. Geophys. Res., 100, 23227–23238, doi:10.1029/95jd02323, 1995.

Plattner, G.-K., Knutti, R., Joos, F., Stocker, T. F., von Bloh, W., Brovkin, V., Cameron, D., Driesschaert, E., Dutkiewicz, S., Eby, M., Edwards, N. R., Fichefet, T., Hargreaves, J. C., Jones, C. D., Loutre, M. F., Matthews, H. D., Mouchet, A., Müller, S. A., Nawrath, S., Price, A., Sokolov, A., Strassmann, K. M., and Weaver, A. J.: Long-term climate commitments projected with climate–carbon cycle models, J. Climate, 21, 2721–2751, 2008.

Prather, M. J.: Lifetimes and time scales in atmospheric chemistry, Philos. T. R. Soc. A, 365, 1705–1726, doi:10.1098/rsta.2007.2040, 2007.

Prather, M. J., Holmes, C. D., and Hsu, J.: Reactive greenhouse gas scenarios: Systematic exploration of uncertainties and the role of atmospheric chemistry, Geophys. Res. Lett., 39, L09803, doi:10.1029/2012gl051440, 2012.

Reisinger, A., Meinshausen, M., Manning, M., and Bodeker, G.: Uncertainties of global warming metrics: CO_2 and CH_4, Geophys. Res. Lett., 37, L14707, doi:10.1029/2010gl043803, 2010.

Reisinger, A., Meinshausen, M., and Manning, M.: Future changes in global warming potentials under representative concentration pathways, Environ. Res. Lett., 6, 024020, doi:10.1088/1748-9326/6/2/024020, 2011.

Rypdal, K., Rive, N., Berntsen, T., Klimont, Z., Mideksa, T., Myhre, G., and Skeie, R. B.: Costs and global impacts of black carbon abatement strategies, Tellus B, 61, 625–641, 2009.

Shindell, D. T.: Evaluation of the absolute regional temperature potential, Atmos. Chem. Phys. Discuss., 12, 13813–13825, doi:10.5194/acpd-12-13813-2012, 2012.

Shindell, D. and Faluvegi, G.: Climate response to regional radiative forcing during the twentieth century, Nat. Geosci., 2, 294–300, 2009.

Shindell, D. T., Faluvegi, G., Koch, D. M., Schmidt, G. A., Unger, N., and Bauer, S. E.: Improved attribution of climate forcing to emissions, Science, 326, 716–718, doi:10.1126/science.1174760, 2009.

Title Page

Abstract | Introduction

Conclusions | References

Tables | Figures

◀ | ▶

◀ | ▶

Back | Close

Full Screen / Esc

Printer-friendly Version

Interactive Discussion

Shine, K. P.: The global warming potential – the need for an interdisciplinary retrail, Climatic Change, 96, 467–472, 2009.

Shine, K. P., Fuglestvedt, J. S., Hailemariam, K., and Stuber, N.: Alternatives to the global warming potential for comparing climate impacts of emissions of greenhouse gases, Climatic Change, 68, 281–302, doi:10.1007/s10584-005-1146-9, 2005.

Shine, K. P., Berntsen, T., Fuglestvedt, J. S., Stuber, N., and Skeie, R. B.: Comparing the climate effect of emissions of short and long lived climate agents, Philos. T. R. Soc. A, 365, 1903–1914, 2007.

Skodvin, T. and Fuglestvedt, J. S.: A comprehensive approach to climate change: Political and scientific considerations, Ambio, 26, 351–358, 1997.

Smith, S. J. and Wigley, T. M. L.: Global warming potentials: 1. Climatic implications of emissions reductions, Climatic Change, 44, 445–457, 2000a.

Smith, S. J. and Wigley, T. M. L.: Global warming potentials: 2. Accuracy, Climatic Change, 44, 459–469, doi:10.1023/a:1005537014987, 2000b.

Stevenson, D. S., Doherty, R. M., Sanderson, M. G., Collins, W. J., Johnson, C. E., and Derwent, R. G.: Radiative forcing from aircraft nox emissions: Mechanisms and seasonal dependence, J. Geophys. Res., 109, D17307, doi:10.1029/2004jd004759, 2004.

Tanaka, K., Peters, G. P., and Fuglestvedt, J. S.: Multi-component climate policy: Why do emission metrics matter?, Carbon Management, 1, 191–197, 2010.

Tanaka, K., Berntsen, T., Fuglestvedt, J. S., and Rypdal, K.: Climate effects of emission standards: The case for gasoline and diesel cars, Environ. Sci. Technol., 46, 5205–5213, doi:10.1021/es204190w, 2012.

Victor, D. G.: Calculating greenhouse budgets, in: Nature, Scientific Correspondence, 431 pp., 1990.

Warren, S. G. and Wiscombe, W. J.: A model for the spectral albedo of snow. Ii: Snow containing atmospheric aerosols, J. Atmos. Sci., 37, 2734–2745, doi:10.1175/1520-0469(1980)037<2734:AMFTSA>2.0.CO;2, 1980.

Wigley, T. M. L.: A simple inverse carbon cycle model, Global Biogeochem. Cy., 5, 373–382, doi:10.1029/91gb02279, 1991.

Wild, O., Prather, M. J., and Akimoto, H.: Indirect long-term global radiative cooling from nox emissions, Geophys. Res. Lett., 28, 1719–1722, doi:10.1029/2000gl012573, 2001.

WMO: Scientific assessment of ozone depletion: 1998, global ozone research and monitoring project, report no. 44, World Meteorological Organization, Geneva, Switzerland, 1999.

Wuebbles, D. J.: Beyond CO_2 – the other greenhouse gases, UCRL-99883, Air and waste management association paper 89-119.4, Livermore National Laboratory, 1989.

Wuebbles, D. J., Jain, A. K., Patten, K. O., and Grant, K. E.: Sensitivity of direct global warming potentials to key uncertainties, Climatic Change, 29, 265–297, doi:10.1007/bf01091865, 1995.

Table 1. Parameters used in the metric equations.

Time horizon (yr)	H
Radiative efficiency (W (m^2 kg)$^{-1}$); RF due to a marginal increase in atmospheric concentration	A_x
Parameters for the exponential Impulse Response Function (IRF) for atmospheric decay of each species	
Weight on each exponential (unitless)	a_i, $\Sigma a_i = 1$
Decay times of each exponential (yr)	τ_i
Number of exponentials (unitless)	I
Parameters of the exponential Impulse Response Function (IRF) of the climate model response to pulse RF	
Components of the climate sensitivity (K (W m^2)$^{-1}$)	c_j, $\lambda = \Sigma c_j$
Decay times due to each component of c_i (yr)	d_j
Number of decay terms (unitless)	J
Ozone-precursor specific parameters	
Radiative efficiency (W (m^2 kg yr)$^{-1}$) for perturbation S	A_{OP}^{S}
Primary mode methane adjustment time (yr)	τ_{PM}
Short-lived ozone lifetime (yr, typically 0.267 yr)	τ_{S}

Table 2. The two methods of calculating radiation efficiency for CO_2 is compared for different steps. The standard step for CO_2 is 1 ppm. The unperturbed concentration here is 378 ppm, which was measured in 2005 (Forster et al., 2007). As Δc increases, the error in the step method increases almost linearly.

Δc step	% Δ from d(RF)/dc to Δc step method
10 ppm	−1.3
1 ppm	−0.13
1 ppb	−1.3e-4
1 ppt	−3.1e-6

Table 3. The top ten emitting countries according to different emission metrics. The percentage given is the share of the global sum.

Ranking of emitters by metrics	GWP20	GWP100	GTP20	GTP50	GTP100
1	US 20.0 %	China 19.2 %	China 19.1 %	China 20.5 %	China 20.9 %
2	China 14.1 %	US 15.7 %	US 14.0 %	US 14.4 %	US 14.7 %
3	Russia 7.8 %	Russia 5.9 %	Russia 6.0 %	Russia 5.3 %	Russia 5.3 %
4	India 6.8 %	India 5.2 %	India 5.8 %	India 4.8 %	India 4.6 %
5	Brazil 6.3 %	Indonesia 4.8 %	Indonesia 4.5 %	Indonesia 4.4 %	Indonesia 4.5 %
6	Indonesia 6.2 %	Brazil 3.6 %	Brazil 4.1 %	Japan 3.1 %	Japan 3.2 %
7	Japan 3.3 %	Japan 3.2 %	Japan 2.7 %	Brazil 2.9 %	Brazil 2.7 %
8	Korea 2.9 %	Korea 2.7 %	Korea 2.2 %	Korea 2.6 %	Korea 2.6 %
9	Germany 2.8 %	Germany 2.4 %	Germany 2.1 %	Germany 2.2 %	Germany 2.4 %
10	France 1.9 %	Canada 1.6 %	Canada 1.5 %	Canada 1.5 %	Canada 1.5 %

Table 4. The share of methane relative to the total emissions for top ten emitters when using different emission metrics. Since some of the SLCFs have a negative climate response, the shares of CH_4 are highest for the shortest time horizon. This is not due to CH_4 dominating the total climate impact, but due to cancellation effects between warming and cooling effects.

Share of methane for countries	GWP20	GWP100	GTP20	GTP50	GTP100
China	103.0 %	23.4 %	42.2 %	9.9 %	3.3 %
US	26.0 %	10.2 %	20.5 %	5.0 %	1.7 %
Russia	62.3 %	25.5 %	44.6 %	12.7 %	4.3 %
India	84.7 %	34.0 %	54.6 %	16.6 %	5.9 %
Indonesia	33.1 %	13.2 %	25.4 %	6.5 %	2.2 %
Japan	11.6 %	3.8 %	8.1 %	1.8 %	0.6 %
Brazil	64.0 %	34.1 %	54.0 %	18.9 %	7.0 %
Germany	19.3 %	7.0 %	14.8 %	3.4 %	1.1 %
Korea	10.1 %	3.4 %	7.5 %	1.6 %	0.5 %
Canada	58.7 %	19.9 %	36.6 %	9.3 %	3.1 %
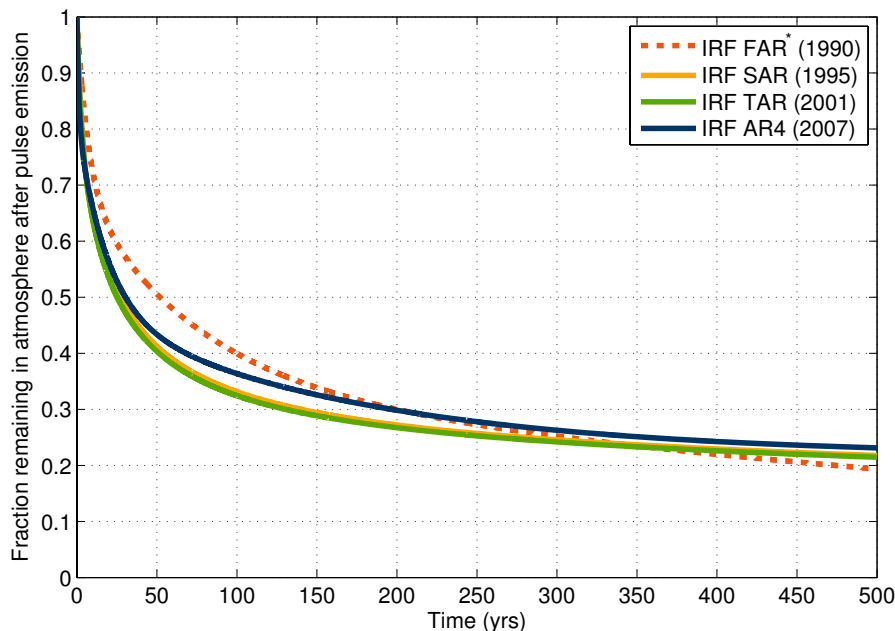
Fig. 1. The Impulse Response Function from the first four IPCC Assessment Reports. The values for the IRFs are from (IPCC, 1994) for FAR, IPCC (1995) for SAR, WMO (1999) for TAR which is the SAR IRF with a different parameterisation, and IPCC (2007) for AR4.The FAR IRF (dotted) is based on an unbalanced carbon-cycle model (ocean only) and, thus, is not directly comparable to the others. The SAR IRF is based the CO_2 response of the Bern model (Bern-SAR), an early generation reduced-form carbon cycle model (Joos et al., 1996), and uses a 10 GtC pulse emission into a constant background without temperature feedbacks (Enting et al., 1994). The IRF was not updated for TAR, but a different parameterisation was used (WMO1999). The AR4 IRF is based on the Bern2.5CC Earth System Model of Interme-diate Complexity (EMIC) (Plattner et al., 2008) and with a pulse size of 40 GtC and includes tempera_Ref327033876.

Title Page

Abstract | Introduction

Conclusions | References

Tables | Figures

◄◄ | ►►

◄ | ►

Back | Close

Full Screen / Esc

Printer-friendly Version

Interactive Discussion
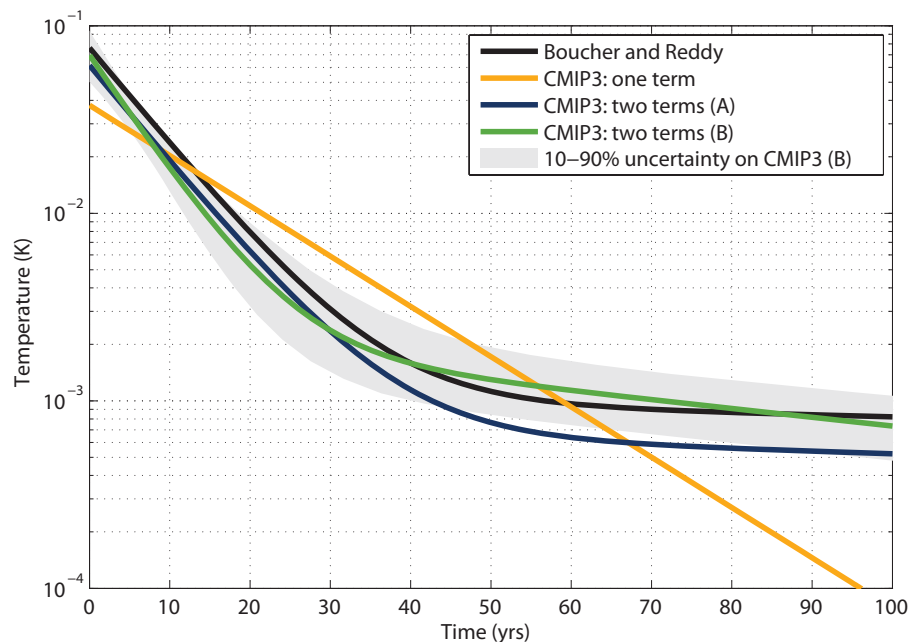
Fig. 2. The temperature response to a unit RF (log scale in temperature) from the Hadley model (Boucher and Reddy, 2008), and the CMIP3 ensemble mean with one exponential term and two exponential terms with different a priori values (Olivié et al., 2012). The IRF A uses an a priori estimate of 10 and 400 yr, while the IRF B uses an a priori estimate of 10 and 100 yr.
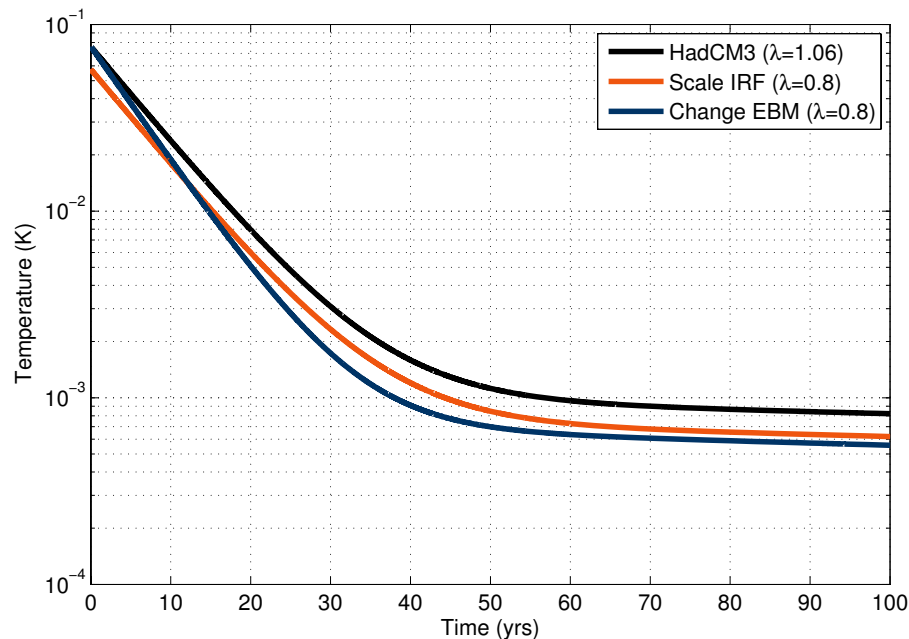
Fig. 3. The IRF from the Hadley model (Boucher and Reddy, 2008) compared to the Hadley IRF (lambda = 1.06) scaled to a climate sensitivity of 0.8 and with the λ changed in a two-layer box-diffusion model.

Fig. 4. A schematic comparison of the two methods to calculate radiative efficiency (RE).
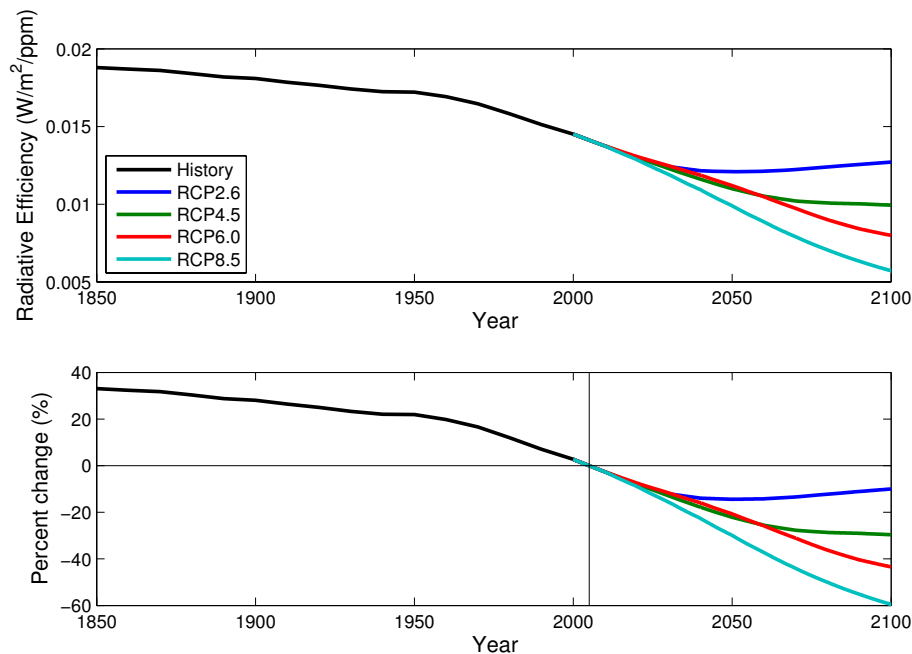
Fig. 5. The radiative efficiency (RE) as a function of concentration for the historic period and the Representative Concentration Pathways (RCPs) to be used in the IPCC Fifth Assessment Report. Constant current (2005) concentrations are represented by the 0 % line.
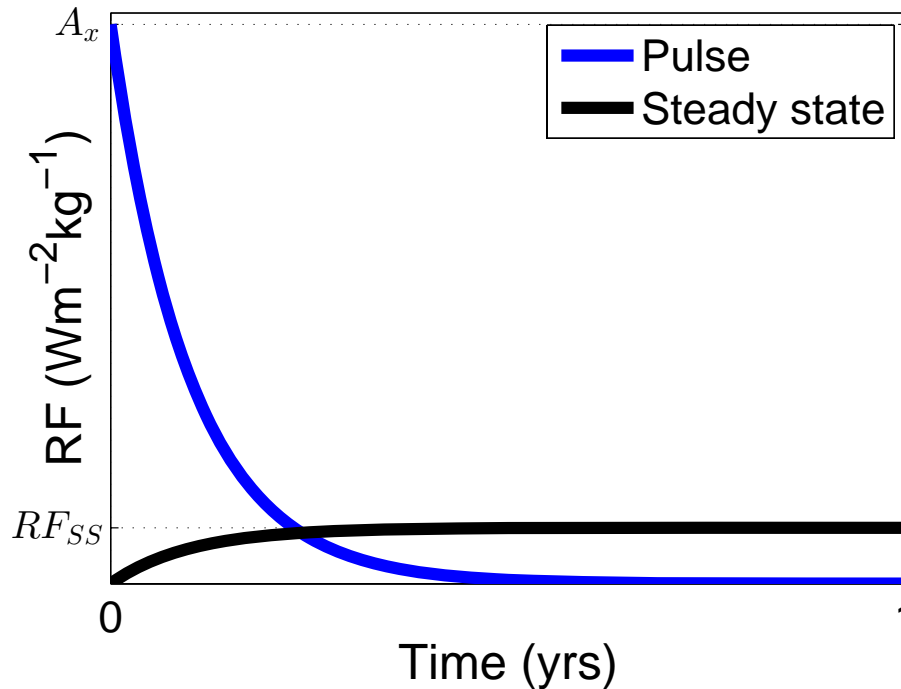
Fig. 6. For SLCF with adjustment times much less than a year, the RF is usually calculated based on a sustained emission, RF_{SS}, and then remapped back to the radiative efficiency, A_x.
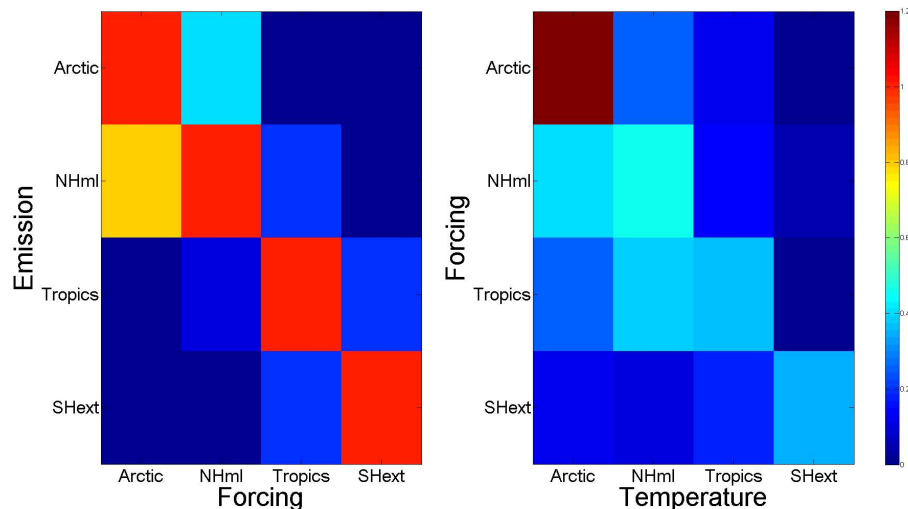
Fig. 7. A schematic regional relationship between emission, RF, and temperature perturbation for SLCFS for the regions: the Southern Hemisphere extratropics (90–28° S, SHext), the tropics (28° S–28° N), the Northern Hemisphere mid-latitudes (28–60° N, NHml), and the Arctic (60–90° N). Values for the emission-RF relationship is inspired by Naik et al. (2005) and the RF-temperature relationship is based on Shindell (2012).
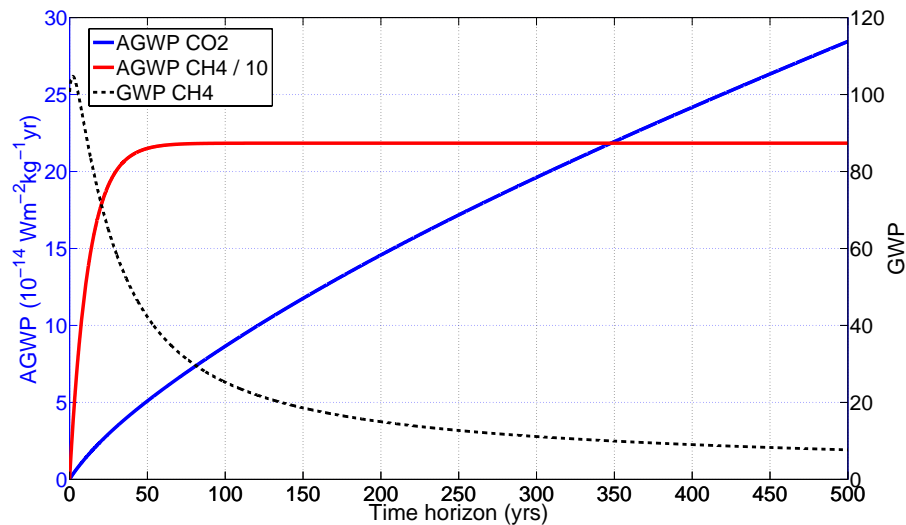
Fig. 8. How GWP for CH_4 is affected by AGWP for both CH_4 and CO_2 with changing time horizons.
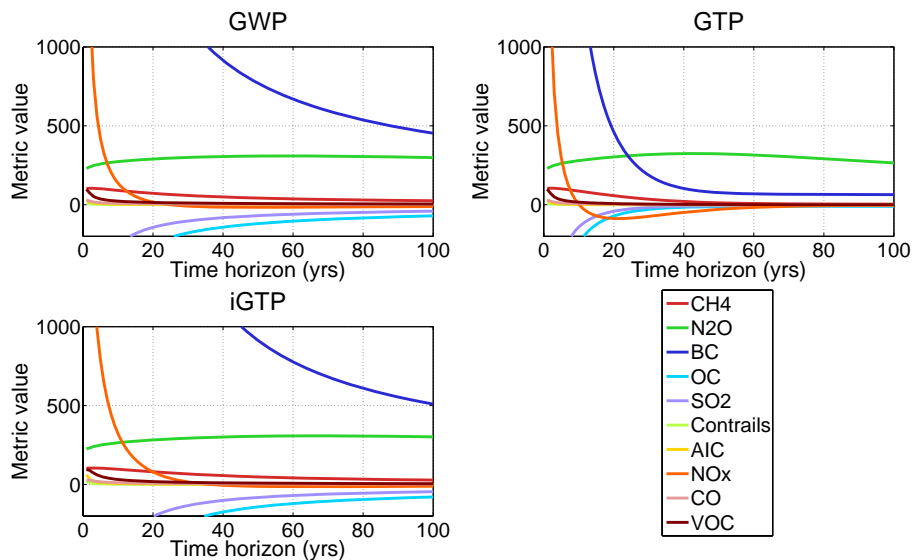
Fig. 9. GWP, GTP, and *i*GTP values for a range of pollutants and time-horizons. The variable time horizon for these metrics GWP($H - t$), GTP($H - t$), and *i*GTP($H - t$), are found be reversing the Time Horizon axis.
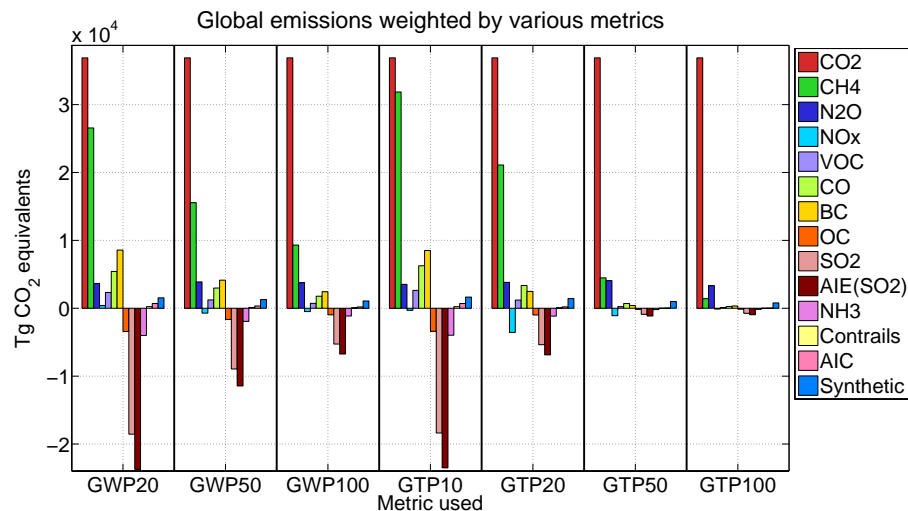
Fig. 10. The weighting of the different emissions from 2008, with BC and OC data from 2005, using various emission metrics.
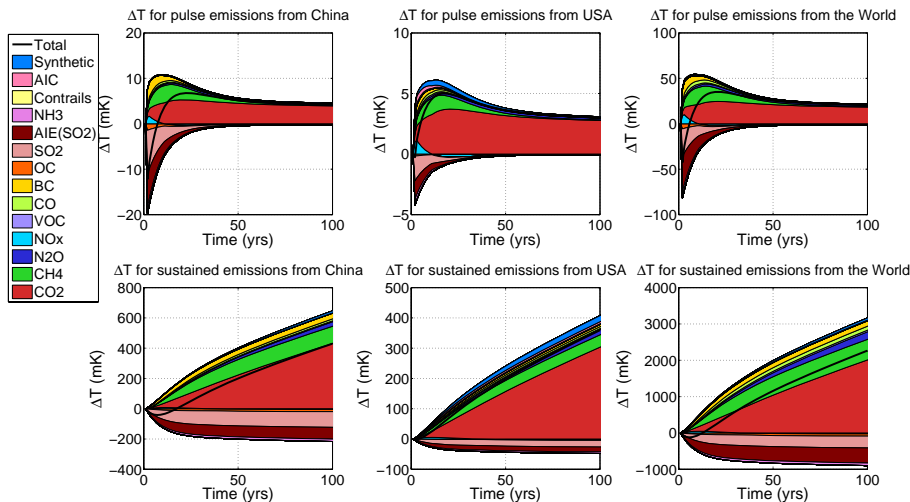
Fig. 11. The estimated temperature perturbation based on AGTP by different species due to EDGAR 2008 emissions. "Synthetic" represents the mainly halogenated hydrocarbons in the Kyoto and Montreal Protocols.
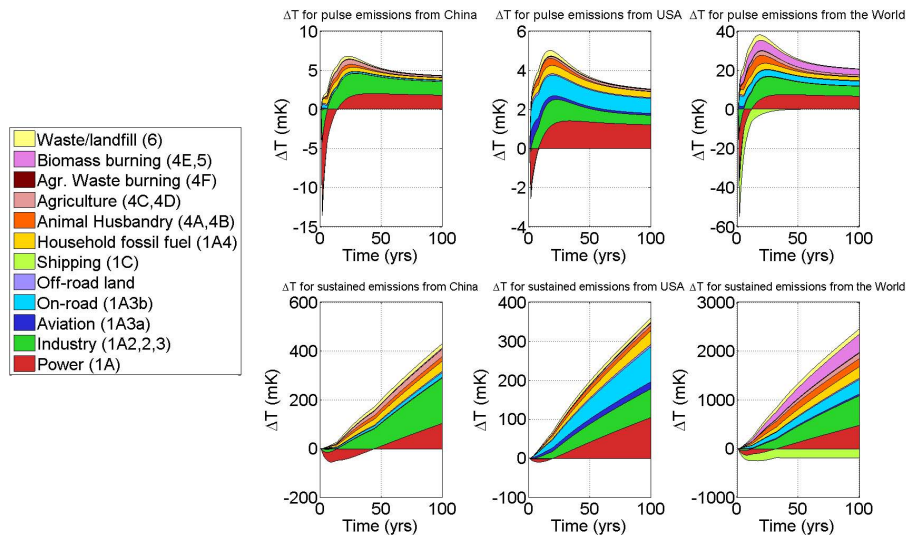
Fig. 12. The estimated temperature perturbation based on AGTP for different sectors due to EDGAR 2008 emissions. The net result (sum of all sectors) is found in Fig. 11.

ΔT(50 years) for pulse emissions from China

ΔT(50 years) for pulse emissions from USA

ΔT(50 years) for pulse emissions from EU

ΔT(50 years) for pulse emissions from the World

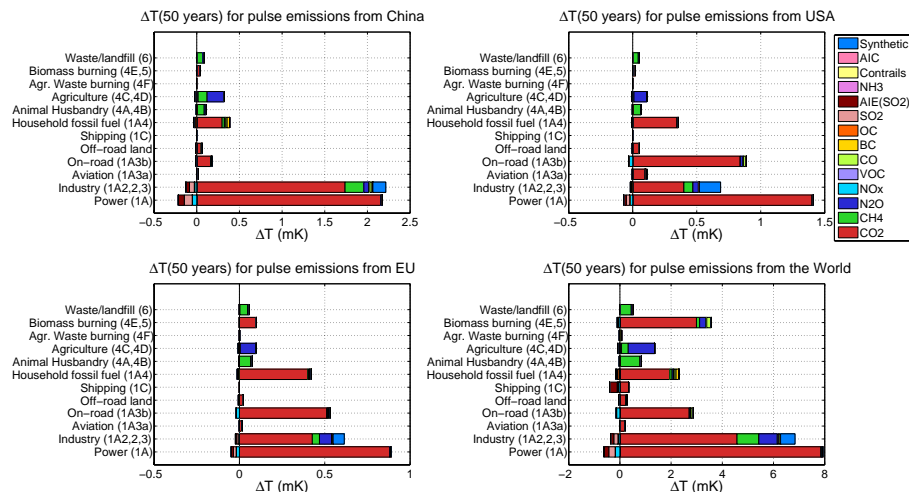Synthetic, AIC, Contrails, NH3, AIE(SO2), SO2, OC, BC, CO, VOC, NOx, N2O, CH4, CO2

Fig. 13. The estimated temperature perturbation based on AGTP 50 yr after EDGAR 2008 emission for different sectors. For a shorter time horizon, the non-CO_2 effects will be relative larger compared to CO_2. "Synthetic" represents the mainly halogenated hydrocarbons in the Kyoto and Montreal Protocols.